earth

MDPI

Article

Climate, Crops, and Communities: Modeling the Environmental Stressors Driving Food Supply Chain Insecurity

Manu Sharma [1,*], Sudhanshu Joshi [2], Priyanka Gupta [1] and Tanuja Joshi [2]

[1] Department of Management Studies, Graphic Era (Deemed to be) University, Dehradun 248002, India; priyankagupta.mgt@geu.ac.in
[2] PM Gati Shakti Centre of Excellence in Logistics and Supply Chain Management, School of Management, Doon University, Dehradun 248001, India; sudhanshujoshi@doonuniversity.ac.in (S.J.); tanujajoshi.phd@doonuniversity.ac.in (T.J.)
* Correspondence: manu.sharma@geu.ac.in

Abstract

As climate variability intensifies, its impacts are increasingly visible through disrupted agricultural systems and rising food insecurity, especially in climate-sensitive regions. This study explores the complex relationships between environmental stressors, such as rising temperatures, erratic rainfall, and soil degradation, with food insecurity outcomes in selected districts of Uttarakhand, India. Using the Fuzzy DEMATEL method, this study analyzes 19 stressors affecting the food supply chain and identifies the nine most influential factors. An Environmental Stressor Index (ESI) is constructed, integrating climatic, hydrological, and land-use dimensions. The ESI is applied to three districts—Rudraprayag, Udham Singh Nagar, and Almora—to assess their vulnerability. The results suggest that Rudraprayag faces high exposure to climate extremes (heatwaves, floods, and droughts) but benefits from a relatively stronger infrastructure. Udham Singh Nagar exhibits the highest overall vulnerability, driven by water stress, air pollution, and salinity, whereas Almora remains relatively less exposed, apart from moderate drought and connectivity stress. Simulations based on RCP 4.5 and RCP 8.5 scenarios indicate increasing stress across all regions, with Udham Singh Nagar consistently identified as the most vulnerable. Rudraprayag experiences increased stress under the RCP 8.5 scenario, while Almora is the least vulnerable, though still at risk from drought and pest outbreaks. By incorporating crop yield models into the ESI framework, this study advances a systems-level tool for assessing agricultural vulnerability to climate change. This research holds global relevance, as food supply chains in climate-sensitive regions such as Africa, Southeast Asia, and Latin America face similar compound stressors. Its novelty lies in integrating a Fuzzy DEMATEL-based Environmental Stressor Index with crop yield modeling. The findings highlight the urgent need for climate-informed food system planning and policies that integrate environmental and social vulnerabilities.

Keywords: environmental stressors; food supply chains; climate change; RCP 4.5 and 8.5

Academic Editor: Dimitrios E. Tsesmelis

Received: 3 August 2025
Revised: 12 September 2025
Accepted: 25 September 2025
Published: 9 October 2025

Citation: Sharma, M.; Joshi, S.; Gupta, P.; Joshi, T. Climate, Crops, and Communities: Modeling the Environmental Stressors Driving Food Supply Chain Insecurity. *Earth* **2025**, *6*, 121. https://doi.org/10.3390/earth6040121

1. Introduction

Global food systems are under increasing pressure as the effects of climate change intensify, resulting in a fragile and progressively insecure food supply chain [1,2]. Across continents, erratic rainfall patterns, rising temperatures, soil degradation, and extreme weather events are troublesome for agricultural productivity, causing fluctuating growing seasons and threatening the stability of rural livelihoods [3]. This convergence of

climate-induced environmental stressors poses complex and systemic risks not only to crop production but also to the entire food supply chain. For many vulnerable communities, especially those in climate-sensitive regions, the growing unpredictability in food availability and access could undermine long-term food security, deepen poverty, and broaden socio-economic inequalities. Food supply chains are multifaceted systems that link agricultural production to market and consumption networks, often spanning local, regional, and global scales [4]. These systems are deeply interconnected and are gradually being exposed to systemic disruptions, particularly those driven by climate variability.

Climate change acts as a stress multiplier by augmenting risks at multiple nodes in the food chain, from on-farm production to transportation and market access. As environmental extremes become more frequent and intense, there is a critical need to understand how different climate-related stressors interact, which ones have the most severe downstream impacts, and how they influence the capacity of agricultural systems to sustain food availability, accessibility, and utilization [5].

Climate and agriculture have a direct and complex relationship. With a change in temperature, crop growth cycles are affected, precipitation patterns are used to determine irrigation demand, and extreme events, such as floods or droughts, may cause the wipe-out of entire harvests [6]. However, these events do not occur in isolation but often in compounding forms, such as when heat stress coincides with water scarcity or when pest outbreaks follow changes in humidity and vegetation dynamics. Even with moderate warming scenarios, significant reductions in crop yields are expected in many global breadbasket regions, particularly for staple crops such as wheat, maize, and rice [7,8]. Moreover, climate stressors affect the agricultural ecosystem beyond crop yields. Soil health deteriorates under prolonged heat and erratic rainfall, while freshwater availability acts as a key resource for irrigation, which is threatened by glacial melt, overuse, and salinization [9]. Pests and diseases are also migrating to unaffected areas due to unstable temperature zones, adding additional challenges to crop management. These biophysical changes translate into disruptions in the food supply chain, affecting logistics, storage, and the predictability of market supply. The most severe impacts are borne by smallholder farmers and low-income consumers, particularly in countries with weak adaptive capacity [10].

Environmental stressors are multifactorial and context-specific. While temperature variances and precipitation variability are prominent, other factors such as sea-level rise, land degradation, desertification, and climate-induced migration are equally influential. The cumulative effect of these stressors is a form of systemic fragility that weakens the resilience of food supply chains. For instance, increased climate-induced migration in rural areas can result in labor shortages during critical harvest periods. Similarly, the demolition of infrastructure due to floods can interrupt cold chain logistics, leading to increased food spoilage and economic losses. Not all stressors impact the system equally or linearly, but some stressors may act as root causes (e.g., persistent droughts that reduce soil fertility), while others may exacerbate existing vulnerabilities. Therefore, it is essential to distinguish between dominant and weak stressors and to evaluate how they interact across temporal and spatial scales. Understanding the structure of these interrelationships is key to developing targeted interventions that enhance food system resilience.

While environmental factors are essential, the human dimensions of food security, namely, access, affordability, and utilization, cannot be overlooked. Vulnerable communities, particularly in low- and middle-income countries, are disproportionately affected by climate-induced food system shocks [7]. These communities often depend on subsistence agriculture, have limited access to adaptive technologies, and are further exposed to food price volatility. Moreover, the loss of crops due to climate stressors may lead to nutritional deficiencies, increased household food insecurity, and may contribute to long-term health

consequences. Socio-economic impacts extend beyond rural households. Urban populations, especially those dependent on food imports or interregional supplies, also face increasing risks due to supply chain disruptions [11]. For example, urban food prices can spike rapidly following climate-induced production shortfalls in nearby rural regions. This interdependence between rural production systems and urban consumption underscores the need for integrated food system models that consider environmental, economic, and social vulnerabilities.

Given the multiplicity of interacting factors, modeling the dynamics of environmental stressors and their cascading impacts on food supply chains requires sophisticated analytical approaches. To address this complexity, this study adopts a Fuzzy Decision-making Trial and Evaluation Laboratory (Fuzzy DEMATEL) approach to analyze the interrelationships and influence structures among key climate-induced environmental stressors. Through this method, we aim to uncover which environmental factors are the most critical drivers of food supply chain disruption, and which ones are more symptomatic or reactive in nature. The research objectives formulated for this study are as follows.

RO1: Identification and categorization of key environmental stressors impacting the stability of food supply chains.

RO2: To establish the cause–effect relationships among the environmental stressors affecting the stability of food supply chains.

RO3: To develop and simulate a composite Environmental Stressor Index (ESI) to assess agricultural vulnerability under current and future climate scenarios (RCP 4.5 and RCP 8.5).

Unlike conventional regression-based models, Fuzzy DEMATEL offers a systems-thinking lens, helping to visualize and quantify the hierarchies of influence among stressors. This is essential for identifying leverage points for intervention areas where policy or technological input can yield the highest systemic resilience gains. Recent evidence has underscored the urgency as, according to [12], approximately 74% of India's rural population remains directly dependent on climate-sensitive agriculture, while [13] warned that South Asia faces among the steepest projected increases in extreme heat events and erratic precipitation by 2050. Uttarakhand, with its fragile Himalayan ecosystems and intensifying anthropogenic pressures, exemplifies these risks, as shown by a 22% increase in reported extreme weather events between 2015 and 2022 [14]. Against this backdrop, the present study aims to develop and apply an ESI to evaluate the composite vulnerability of food supply chains under climate variability and change. Specifically, we investigate three districts, Rudraprayag, Udham Singh Nagar, and Almora, as representative cases of diverse agro-ecological and socio-economic contexts. This paper addresses the cause–effect relationships among environment stressors and identifies the most prominent and influenced stressors to be considered for simulation under RCP 4.5 and 4.8 scenarios.

2. Trends in Climate

The historical patterns in the summer maximum and the winter minimum temperatures, as well as rainfall, from 1990 to 2019 are analyzed and reported by the Center for Study of Science, Technology, and Policy [14,15]. The report shows that there is an increase of up to 0.9 °C in the summer maximum temperature and 0.5 °C in the winter minimum temperature in all districts of India [Prajapati]. Also, a warming of up to 0.5 °C is recorded in 70% of the districts of India. Warming in the northern states is higher compared to the southern states. The highest warming of 0.5–0.9 °C is recorded in 54% of districts of India, including those in the northern states of Punjab, Haryana, Uttarakhand, Uttar Pradesh, and Bihar, the western states of Rajasthan and Gujarat, as well as the north-eastern states [15,16].

During this historical period, there is a noticeable increasing trend in rainfall during the Kharif season (June to September) across all districts of India. Overall, rainfall increases by up to 15% during this period. The highest increase, ranging from 10% to 15%, is observed in the northeastern states, specifically in districts of Arunachal Pradesh, Sikkim, Meghalaya, and northern Nagaland, as well as in the Western Ghats districts of southern India [17]. A moderate increase of 5% to 10% is recorded in approximately 20% of India's districts, including parts of Bihar, Chhattisgarh, Odisha, Jharkhand, and the majority of Madhya Pradesh. A smaller increase, ranging from 1% to 5%, is observed in about 45% of districts, notably in Karnataka, Tamil Nadu, Telangana, Andhra Pradesh, and the northern states of Haryana and Punjab, along with the western regions of Rajasthan and Gujarat [14,15]. A warming of 1 °C to 2.5 °C is projected for a majority of districts compared to the historical period, considering both RCP 4.5 and RCP 8.5 scenarios. A warming of >1 °C is projected for a majority of districts compared to the historical period, considering both RCP 4.5 and RCP 8.5 scenarios [18,19].

2.1. District-Level Climate Projections Under RCP 4.5 and RCP 8.5 Scenarios

Under the RCP 4.5 scenario, a moderate warming trend is apparent across most Indian districts. Approximately 72% of districts are projected to experience a temperature rise between 1 °C and 1.5 °C. A total of 15% of districts may see warming between 1.5 °C and 2 °C. Only 2% of districts will likely warm by 2 °C to 2.5 °C, while a few isolated districts (1%), such as Nashik and Jalgaon in Maharashtra, are projected to face the highest warming in the range of 2.5 °C to 3 °C. A total of 11% of districts are accurately projected to see 1 °C warming, while 13% of districts may experience less than 1 °C warming, especially in parts of Karnataka and Rajasthan. Regionally, 1.5 °C to 2 °C warming is likely in some districts of Uttarakhand, Uttar Pradesh, Arunachal Pradesh, and Tamil Nadu. In terms of Kharif season rainfall, 35% of districts are anticipated to experience a moderate increase of 10–15%, mostly in states such as Karnataka, Tamil Nadu, Kerala, Odisha, and West Bengal. About 18% of districts could see an increase of 15–25%, while only 2% of districts may see a significant rise of 25–35% in rainfall, including parts of Maharashtra, Gujarat, and Bihar. However, 45% of districts are projected to have less than a 10% increase in Kharif rainfall, signifying localized rainfall escalation rather than uniform increases. High-intensity rainfall events are predicted to increase in various states including Maharashtra, Chhattisgarh, Uttar Pradesh, and Himachal Pradesh, though these changes remain scattered [18–20].

In the RCP 8.5 scenario, it is assumed that there will be higher emissions and less mitigation leading to a more intense warming pattern. In total, 63% of districts are projected to warm by 1.5 °C to 2 °C, while 15% may experience warming above 2 °C. An additional 2% of districts may warm between 2 °C and 2.5 °C. Extreme warming (2.5 °C to 3 °C) is anticipated in specific districts such as Amravati, Jalna, Chandel, and Pherzawl, with some districts possibly exceeding 3 °C. Approximately 17% of districts may warm by 1 °C to 1.5 °C, with only 3% experiencing precisely 1 °C, and 6% experiencing less than 1 °C. Warming is more widespread and severe under RCP 8.5, extensively affecting regions in Maharashtra, Manipur, Karnataka, and Gujarat [18]. Rainfall patterns under RCP 8.5 also show stronger shifts, where 9% of districts could see a 25–35% increase in Kharif season rainfall, with this trend extending to all districts in Tamil Nadu, Telangana, Gujarat, and Himachal Pradesh. A significant 50% of districts are anticipated to experience rainfall increases of 15–25%, while 25% may experience a 10–15% increase. RCP 8.5 leads to higher and more widespread warming and rainfall variability compared to RCP 4.5. The implications are significant for regional planning, agricultural resilience, and climate adaptation strategies, especially in hotspot regions such as Maharashtra, Northeast India, and central

plains; these areas face both rising temperatures and altered precipitation patterns under both scenarios.

2.2. Environmental Stressors

2.2.1. Climatic Stressors

Rising temperatures, particularly in tropical countries like India, pose major risks to agriculture, health, and biodiversity. This rise has already reduced wheat yields and increased heat-related illnesses [18]. Increasing variability in monsoon onset, duration, and intensity has disrupted crop cycles and water management. Rainfall variability contributes to both drought and flood risks, with uneven spatial and temporal distribution [19]. India has seen a higher frequency of meteorological and hydrological droughts due to erratic precipitation and rising evapotranspiration [21]. This affects groundwater recharge and crop productivity. Flash floods and riverine floods have become more common due to urbanization and intense rainfall [22,23]. The Himalayan region and Indo-Gangetic plains remain particularly vulnerable [22].

2.2.2. Land Use Stressors

Urbanization leads to the loss of agricultural and forest lands. Between 2001 and 2020, built-up areas increased by over 50%, contributing to the urban heat island effect and habitat loss. Soil fertility is declining due to over-cultivation, deforestation, and chemical overuse. About 30% of India's total land is degraded [24]. Irrigation mismanagement and groundwater overuse have caused salinity in soils, particularly in Punjab, Gujarat, and coastal Andhra Pradesh [24]. While warming is dominant, unseasonal cold spells still affect rabi crops and horticulture, especially in the northwestern and central highlands [25,26].

2.2.3. Hydrological Stressors

The Water Stress Index has worsened in arid zones like Rajasthan and Bundelkhand. Increased demand and reduced monsoon reliability exacerbate water conflicts [26,27]. India is the largest extractor of groundwater globally. Critical regions such as Punjab, Haryana, and parts of Tamil Nadu face alarming depletion. Heatwaves have become longer and more intense, particularly in central and western India [28,29]. They contribute to labor productivity loss and mortality [30]. Changing temperature and humidity patterns facilitate pest outbreaks (e.g., locusts, fall armyworm) and vector-borne diseases like dengue and malaria.

2.2.4. Ecological Stressors

India has seen significant forest cover loss due to mining, infrastructure projects, and shifting cultivation, particularly in the northeast and central tribal regions [31,32]. Cyclones, cloudbursts, and hailstorms have intensified, with events like Cyclone Amphan and Uttarakhand cloudbursts causing extensive socio-economic damage. India's 7500 km coastline faces sea-level rises, especially in Sundarbans, Chennai, and Mumbai, affecting livelihoods and mangrove ecosystems. Rising temperatures and dry spells are increasing the frequency of forest fires, especially in Uttarakhand, Odisha, and Andhra Pradesh [33].

The stressors are shown in Table 1.

During 1990–2019, India experienced a significant warming trend, with summer maximum and winter minimum temperatures rising by up to 0.9 °C and 0.5 °C, respectively; northern and northeastern states recorded the highest increases. Rainfall during the Kharif season rose by up to 15%, with the sharpest increases observed in the northeastern states and the Western Ghats. Future climate projections indicate further warming of 1–2.5 °C across most districts under both RCP 4.5 and RCP 8.5 scenarios. RCP 8.5 shows more widespread and severe warming, particularly in Maharashtra, the Northeast, and central plains, alongside substantial rainfall variability. These climatic changes are compounded by

environmental stressors such as droughts, floods, groundwater depletion, soil degradation, urbanization, extreme weather events, and sea-level rise. In conjunction, these factors pose severe risks to India's agriculture, food supply chains, water security, ecosystems, and livelihoods, emphasizing the urgent need for adaptive and resilient strategies.

Table 1. List of environmental stressors.

	Environment Stressors	Definition/Description	Impact on Food Supply Chains	Key Sources
ES1	Temperature Rise	Long-term increase in mean surface temperatures	Reduces crop yields, shortens growing seasons, increases water demand, affects cold storage efficiency	[10]
ES2	Rainfall Variability	Fluctuation in amount, intensity, or timing of rainfall	Disrupts planting schedules, irrigation planning, and crop growth, leads to unpredictable harvests	[15–17]
ES3	Drought Frequency	Increased occurrence of periods with below-average precipitation	Causes water scarcity, crop failure, and livestock stress, disrupts upstream supply of raw materials	[18,19]
ES4	Flood Events	Inundation of land from rainfall, river overflow, or coastal surges	Destroys crops, damages rural infrastructure, roads, and storage, delays food distribution	[22,23]
ES5	Soil Degradation	Decline in soil quality due to erosion, salinization, nutrient loss	Reduces crop productivity, increases input costs (fertilizer/ irrigation), undermines long-term agricultural sustainability	[23,24]
ES6	Groundwater Depletion	Decline in aquifer levels due to over-extraction	Limits irrigation potential, raises cost of water extraction, increases reliance on erratic surface water	[27]
ES7	Water Stress Index	Ratio of water demand to renewable water availability	Indicates systemic risk of irrigation failure, affects food processing operations needing water	[27]
ES8	Heatwaves	Prolonged periods of extreme heat	Impacts crop pollination, increases post-harvest losses, affects farm labor productivity	[28,29]
ES9	Pest and Disease Outbreaks	Increase in crop pests and diseases due to warming and humidity changes	Leads to production losses, increased use of pesticides, trade restrictions	[10]
ES10	Land-Use Change/Urban Sprawl	Conversion of farmland to urban or industrial use	Shrinks agricultural area, fragments food production systems, causes logistical delays	[26,27]
ES11	Vegetation Loss (NDVI Decline)	Reduction in plant biomass or greenness detected via satellite (e.g., NDVI)	Indicates stress on croplands, pasture areas, and forest–farm interface zones	[31–34]
ES12	Extreme Weather Events (Cyclones, Hailstorms)	High-intensity weather hazards disrupt local ecosystems	Damages standing crops, logistics, infrastructure, cold chains, and supply coordination	[26,27]
ES13	Sea-Level Rise/ Coastal Erosion	Submergence and salinization of coastal agricultural zones	Affects rice, coconut, aquaculture, disrupts port-based food logistics	[34]
ES14	Air Pollution (Tropospheric Ozone)	Reduces crop productivity by damaging leaf tissues and photosynthesis	Lowers yield quality and quantity, contributes to long-term ecosystem degradation	[35]
ES15	Forest Fires/ Biomass Burning	Climate-induced or anthropogenic fires degrading large swaths of agricultural interface	Destroys crops, degrades soil, reduces labor availability, delays transport	[36]
ES16	Salinization/Alkalinity	Accumulation of salts in soil and water bodies	Reduces soil fertility and water usability, prevalent in irrigated drylands	[34]

Table 1. *Cont.*

	Environment Stressors	Definition/Description	Impact on Food Supply Chains	Key Sources
ES17	Cold Spells/ Frost Events	Unseasonal cold temperatures affecting crop physiology	Impacts flowering, delays harvest, affects fruits and vegetables	[36]
ES18	Digital Infrastructure Gaps	Lack of precision weather monitoring, early warning systems, and ICT tools	Limits climate-smart decision making and supply chain responsiveness	[37–40]
ES19	Transport and Energy Disruption	Indirect environmental stress due to floods, storms, or heat damaging roads/grids	Affects cold chains, food storage, and delivery networks	[38]

3. Methods

The Fuzzy DEMATEL approach improves the assessment of equivocal empirical data. By employing fuzzy logic, decision-makers can evaluate alternatives based on high, medium, and low assessment levels. Fuzzy DEMATEL, with its causal diagram architecture, enables decision-makers to pinpoint essential success determinants, hence improving the systematic analysis of the situation [38]. This strategy exceeds other multi-criteria decision-making approaches in decision-making systems. Fuzzy-DEMATEL demonstrates greater effectiveness than hierarchical approaches in discerning complex interrelations across many systems, notwithstanding its application in the implementation phase. Fuzzy DEMATEL exhibits adaptability and responsiveness in decision-making, offering benefits to intricate information systems with adaptable decision-making capacities. Table 2 outlines the linguistic scales utilized by the experts to generate their paired evaluations during the investigation.

Table 2. Fuzzy labels.

Terms	Score	Triangular Fuzzy Values
Very High Influence (VH)	4	(0.75, 1.0, 1.0)
High Influence (H)	3	(0.5, 0.75, 1.0)
Low Influence (L)	2	(0.25, 0.5, 0.75)
Very Low Influence (VL)	1	(0, 0.25, 0.5)
No Influence (No)	0	(0, 0, 0.25)

A structured flow chart for the methodology undertaken is shown in Figure 1.

The criteria for selecting climate data is based on (i) use of CMIP6 multi-model ensemble projections to ensure the latest generation of scenarios, (ii) bias correction and downscaling to district-level resolution, and (iii) consistent temporal coverage with historical IMD datasets for calibration (1980–2019) and projection (2020–2100). A questionnaire is designed for experts to conduct pairwise comparisons before Fuzzy DEMATEL implementation. Information on the 15 experts contributing to this study is shown in Table 3.

Table 3. Expert details.

Experts	Designation, Area of Expertise	Experience
E1	Environmental Scientist	10+ years
E2	Climatologist/Climate Scientist	5+ years
E3	Agricultural Scientist	5+ years

Table 3. *Cont.*

Experts	Designation, Area of Expertise	Experience
E4	Hydrologist/Water Resource Expert	8+ years
E5	Environmental Scientist	5+ years
E6	Public Policy Expert (Agro-climatic focus)	8+ years
E7	Soil Scientist	10+ years
E8	Remote Sensing and GIS Expert	6+ years
E9	Environmental Scientist	8+ years
E10	Food Systems Expert	10+ years
E11	Agro-Supply Chain Expert	10+ years
E12	Environmental Scientist	8+ years
E13	Environmental Scientist	5+ years
E14	Agro-Supply Chain Expert	8+ years
E15	Agro-Supply Chain Expert	10+ years

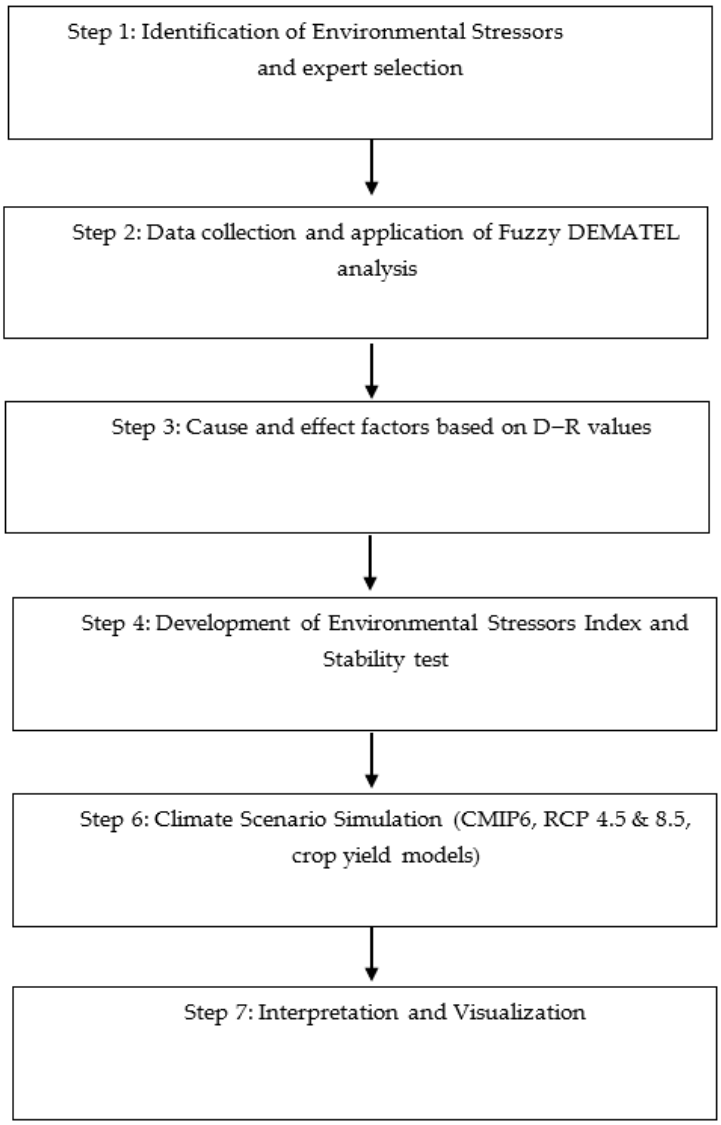

Figure 1. Flowchart for methodology.

3.1. Steps for F-DEMATEL

The F-DEMATEL approach is employed to analyze influencing aspects inside a complex system, offering a structured framework to investigate the interconnections among different elements. The essential steps are as follows:

Step 1: Ask each expert to provide assessment on five levels of 1–5 including Very High Influence (VH); High Influence (H); Low Influence (L); Very Low Influence (VL); No Influence (No).

Step 2: Develop the initial direct matrix based on the score provided by the experts.

Step 3: Employ Table 2 to convert the linguistic scale into triangular fuzzy integers.

Step 4: The CSCF method is employed to fuzzy variables to compute the weighted average.

Step 5: Obtaining fuzzy direct relation matrix Z = $\left[Z_{ij}\right]_{n\times n}$.

$$xl_{ij}^{k} = (l_{ij}^{k} - minl_{ij}^{k}) / \triangle_{min}^{max} \tag{1}$$

$$xm_{ij}^{k} = (m_{ij}^{k} - minl_{ij}^{k}) / \triangle_{min}^{max} \tag{2}$$

$$xr_{ij}^{k} = (r_{ij}^{k} - minl_{ij}^{k}) / \triangle_{min}^{max} \tag{3}$$

$$\text{where } \triangle_{min}^{max} = maxr_{ij}^{k} - minl_{ij}^{k} \tag{4}$$

Step 6: Constructing the normalized direct relation matrix.

$$m = min[\frac{1}{max\sum_{j=1}^{n}|aij|}, \frac{1}{max\sum_{j=1}^{n}|aij|}] \tag{5}$$

Integrating crisp value through the following equation.

$$Z_{ij} = \frac{1}{p}\left(z_{ij}^{1} + Z_{ij}^{2} + Z_{ij}^{p}\right) \tag{6}$$

Step 7: Formation of the total relation matrix.

The total of an uninterrupted series of direct and indirect influences among elements is computed as a geometric propagation according to graph theory principles. The total of this progression constitutes the matrix of the generic relation *T*, where I represents an $n \times n$ identity matrix.

$$T = N(I - N)^{-1} \tag{7}$$

Step 9: Calculating the scores of row sums (D) and column sums (R).

$$D = \left[\sum_{j=1}^{n} t_{ij}\right]_{nX1} \tag{8}$$

$$R = \left[\sum_{i=1}^{n} t_{ij}\right]_{1Xn} \tag{9}$$

3.2. Development of Environmental Stressors Index

The ESI is a composite metric developed to quantify and assess the cumulative impact of various environmental stressors on vulnerable systems, particularly the food supply chain. Based on the results from Fuzzy DEMATEL, weights are obtained and normalized to create dimensionless indicators for each stressor. The ESI developed in this study is a static composite indicator inspired by causal structures. The use of Fuzzy DEMATEL (D + R) ensures that stressors with higher systemic importance receive greater weight in the index. Its design is a weighted aggregation framework rather than a dynamic systems model. The ESI thus serves as a decision-support tool to identify climate hotspots, guide risk prioritization, and support targeted interventions in policy and planning for

climate resilience, particularly in food-insecure regions. The normalization process in this study uses a uniform min–max scaling baseline across all regions and years. Specifically, X_{min} and X_{max} values are determined from the entire dataset (1980–2019 baseline and 2020–2100 projections) rather than from region-specific subsets, ensuring comparability across districts and scenarios. The normalized values thus fall between 0 and 1, where 1 indicates the most adverse condition observed in the sample and 0 the least. To address indicator directionality, variables are classified into two categories: negative stressors (e.g., temperature rise, drought frequency, etc.), where higher values imply greater vulnerability, are normalized directly; in the case of positive stressors (e.g., infrastructure accessibility, internet penetration), where higher values imply reduced vulnerability, reverse normalization is applied.

The steps are as follows:

Step 1: Identify relevant stressors;

Step 2: Assign weights using Fuzzy DEMATEL centrality (D + R);

Step 3: Normalize the weights using Equation (9)

$$\frac{(\boldsymbol{D}+\boldsymbol{R})\boldsymbol{i}}{\sum \boldsymbol{i}=1\boldsymbol{n}(\boldsymbol{D}+\boldsymbol{R})\boldsymbol{i}} \tag{10}$$

Step 4: Collect and normalize stressor data (X_n)

For each region or grid cell (e.g., districts), gather actual values of each stressor. For instance,

$$Xnorm = \frac{\boldsymbol{X}-\boldsymbol{Xmin}}{\boldsymbol{Xmax}-\boldsymbol{Xmin}} \tag{11}$$

Step 5: Compute composite Environmental Stressor Index (ESI)

$$\text{ESI} = \sum_{i=1}^{k} \boldsymbol{Wi}\ Xnorm, i \tag{12}$$

Step 6: Interpretation of the ESI Scores;

Step 7: Visualize the ESI.

3.3. Penalty-Adjusted ESI

To reduce risk of multicollinearity and potential double-counting of highly correlated stressors, a penalty-adjusted weighting scheme is introduced in the construction of the ESI. Each indicator's weight is rescaled according to the sum of its absolute correlations with other indicators, so that indicators with stronger redundancy are down weighted. The penalized weights are then normalized to sum to one and used to recalculate ESI scores for Rudraprayag, Udham Singh Nagar, and Almora.

4. Results and Discussion

Fuzzy DEMATEL analysis is conducted to understand the causal relationships among 19 environmental stressors affecting food supply chain insecurity. By evaluating the cause–effect dynamics through fuzzy logic and expert input, this study classifies factors into two key groups—the cause group (influential factors) and the effect group (influenced factors). The initial direct-relation matrix (Z) is created using Equations (1)–(4), developed based on expert responses applying the linguistic scale outlined in Table 2. The fuzzy direct relation matrix is derived from Equations (5) and (6). Equations (7)–(10) yield a comprehensive relation matrix, as presented in Table 4.

Table 4. Total-relation matrix.

Total-Relation matrix T for first component of a fuzzy number (l)																			
ES1	0.0338	0.0701	0.0638	0.0615	0.0759	0.0611	0.0627	0.0661	0.0569	0.0740	0.0792	0.0533	0.0795	0.0471	0.0788	0.0559	0.0740	0.0492	0.0677
ES2	0.0483	0.0255	0.0365	0.0403	0.0522	0.0374	0.0531	0.0423	0.0685	0.0569	0.0718	0.0443	0.0713	0.0370	0.0681	0.0430	0.0698	0.0380	0.0717
ES3	0.0589	0.0438	0.0301	0.0415	0.0620	0.0386	0.0655	0.0543	0.0595	0.0704	0.0625	0.0674	0.0614	0.0644	0.0614	0.0701	0.0611	0.0438	0.0628
ES4	0.0652	0.0474	0.0443	0.0265	0.0770	0.0392	0.0586	0.0526	0.0618	0.0672	0.0757	0.0626	0.0741	0.0454	0.0728	0.0600	0.0562	0.0520	0.0769
ES5	0.0516	0.0514	0.0373	0.0461	0.0273	0.0459	0.0505	0.0356	0.0418	0.0463	0.0640	0.0511	0.0427	0.0392	0.0442	0.0430	0.0426	0.0381	0.0488
ES6	0.0687	0.0536	0.0697	0.0534	0.0606	0.0234	0.0433	0.0411	0.0584	0.0564	0.0623	0.0700	0.0735	0.0413	0.0721	0.0490	0.0647	0.0446	0.0712
ES7	0.0486	0.0412	0.0541	0.0379	0.0578	0.0469	0.0241	0.0511	0.0404	0.0559	0.0515	0.0474	0.0595	0.0418	0.0700	0.0478	0.0662	0.0374	0.0578
ES8	0.0731	0.0561	0.0507	0.0529	0.0785	0.0500	0.0398	0.0279	0.0599	0.0735	0.0622	0.0485	0.0722	0.0657	0.0637	0.0686	0.0686	0.0658	0.0744
ES9	0.0541	0.0650	0.0706	0.0409	0.0760	0.0408	0.0428	0.0272	0.0308	0.0603	0.0729	0.0703	0.0733	0.0544	0.0710	0.0592	0.0719	0.0522	0.0578
ES10	0.0547	0.0664	0.0595	0.0632	0.0636	0.0629	0.0669	0.0385	0.0690	0.0302	0.0625	0.0589	0.0489	0.0495	0.0505	0.0523	0.0480	0.0354	0.0724
ES11	0.0546	0.0528	0.0554	0.0454	0.0697	0.0489	0.0495	0.0395	0.0450	0.0423	0.0320	0.0697	0.0707	0.0510	0.0600	0.0575	0.0367	0.0602	0.0707
ES12	0.0499	0.0393	0.0443	0.0363	0.0439	0.0384	0.0423	0.0619	0.0655	0.0405	0.0419	0.0255	0.0571	0.0496	0.0567	0.0520	0.0560	0.0472	0.0574
ES13	0.0558	0.0416	0.0655	0.0382	0.0682	0.0369	0.0657	0.0539	0.0454	0.0689	0.0454	0.0674	0.0306	0.0388	0.0712	0.0572	0.0474	0.0486	0.0580
ES14	0.0616	0.0431	0.0507	0.0381	0.0705	0.0350	0.0430	0.0369	0.0653	0.0418	0.0693	0.0421	0.0419	0.0219	0.0441	0.0659	0.0653	0.0385	0.0451
ES15	0.0514	0.0605	0.0601	0.0659	0.0635	0.0465	0.0403	0.0560	0.0587	0.0724	0.0643	0.0722	0.0747	0.0401	0.0347	0.0730	0.0730	0.0520	0.0763
ES16	0.0605	0.0545	0.0663	0.0529	0.0732	0.0608	0.0459	0.0551	0.0700	0.0605	0.0744	0.0596	0.0491	0.0392	0.0585	0.0295	0.0467	0.0299	0.0756
ES17	0.0476	0.0618	0.0601	0.0611	0.0489	0.0380	0.0518	0.0529	0.0431	0.0458	0.0497	0.0419	0.0666	0.0621	0.0573	0.0404	0.0283	0.0361	0.0590
ES18	0.0582	0.0449	0.0536	0.0438	0.0760	0.0402	0.0537	0.0555	0.0580	0.0463	0.0738	0.0563	0.0724	0.0544	0.0738	0.0704	0.0703	0.0250	0.0633
ES19	0.0632	0.0452	0.0662	0.0436	0.0783	0.0406	0.0668	0.0678	0.0720	0.0699	0.0761	0.0616	0.0545	0.0442	0.0542	0.0622	0.0615	0.0648	0.0357

Table 4. *Cont.*

Total-Relation matrix T for first component of a fuzzy number (m)																			
ES1	0.0438	0.0823	0.0771	0.0728	0.0883	0.0742	0.0759	0.0791	0.0715	0.0869	0.0911	0.0673	0.0916	0.0611	0.0907	0.0654	0.0876	0.0618	0.0714
ES2	0.0662	0.0382	0.0531	0.0570	0.0659	0.0558	0.0696	0.0569	0.0823	0.0720	0.0857	0.0623	0.0854	0.0564	0.0852	0.0611	0.0827	0.0565	0.0848
ES3	0.0753	0.0631	0.0441	0.0605	0.0806	0.0598	0.0836	0.0704	0.0768	0.0868	0.0800	0.0851	0.0792	0.0807	0.0788	0.0859	0.0767	0.0603	0.0801
ES4	0.0831	0.0636	0.0660	0.0396	0.0915	0.0602	0.0754	0.0689	0.0773	0.0828	0.0908	0.0771	0.0891	0.0580	0.0885	0.0759	0.0726	0.0705	0.0895
ES5	0.0671	0.0686	0.0572	0.0637	0.0400	0.0630	0.0659	0.0542	0.0582	0.0603	0.0805	0.0677	0.0615	0.0530	0.0615	0.0578	0.0617	0.0541	0.0619
ES6	0.0848	0.0746	0.0859	0.0706	0.0803	0.0379	0.0636	0.0617	0.0774	0.0786	0.0800	0.0871	0.0901	0.0599	0.0881	0.0694	0.0689	0.0604	0.0871
ES7	0.0580	0.0584	0.0702	0.0564	0.0748	0.0653	0.0371	0.0671	0.0608	0.0718	0.0707	0.0626	0.0791	0.0572	0.0838	0.0610	0.0815	0.0565	0.0730
ES8	0.0876	0.0753	0.0678	0.0725	0.0940	0.0693	0.0628	0.0420	0.0792	0.0893	0.0807	0.0683	0.0875	0.0825	0.0814	0.0882	0.0845	0.0803	0.0901
ES9	0.0749	0.0817	0.0865	0.0611	0.0911	0.0600	0.0642	0.0518	0.0456	0.0771	0.0910	0.0878	0.0909	0.0712	0.0888	0.0784	0.0875	0.0714	0.0721
ES10	0.0589	0.0808	0.0742	0.0781	0.0790	0.0782	0.0819	0.0592	0.0852	0.0431	0.0785	0.0747	0.0676	0.0656	0.0671	0.0707	0.0645	0.0543	0.0853
ES11	0.0730	0.0703	0.0750	0.0603	0.0846	0.0679	0.0669	0.0601	0.0646	0.0646	0.0465	0.0850	0.0877	0.0683	0.0786	0.0739	0.0590	0.0751	0.0856
ES12	0.0599	0.0572	0.0573	0.0541	0.0583	0.0538	0.0594	0.0763	0.0806	0.0602	0.0630	0.0383	0.0732	0.0653	0.0725	0.0685	0.0722	0.0647	0.0728
ES13	0.0655	0.0633	0.0830	0.0583	0.0857	0.0576	0.0815	0.0697	0.0646	0.0847	0.0669	0.0842	0.0450	0.0580	0.0865	0.0734	0.0606	0.0674	0.0722
ES14	0.0797	0.0610	0.0666	0.0575	0.0854	0.0553	0.0581	0.0563	0.0812	0.0609	0.0852	0.0609	0.0641	0.0344	0.0633	0.0803	0.0815	0.0491	0.0642
ES15	0.0681	0.0775	0.0799	0.0824	0.0817	0.0681	0.0630	0.0739	0.0793	0.0894	0.0825	0.0892	0.0924	0.0622	0.0499	0.0882	0.0886	0.0732	0.0906
ES16	0.0840	0.0720	0.0829	0.0698	0.0892	0.0780	0.0636	0.0718	0.0859	0.0775	0.0904	0.0766	0.0694	0.0598	0.0787	0.0435	0.0658	0.0506	0.0890
ES17	0.0631	0.0775	0.0783	0.0760	0.0704	0.0557	0.0695	0.0675	0.0639	0.0638	0.0665	0.0621	0.0859	0.0773	0.0752	0.0619	0.0414	0.0561	0.0749
ES18	0.0641	0.0655	0.0713	0.0616	0.0898	0.0604	0.0714	0.0720	0.0758	0.0659	0.0884	0.0748	0.0868	0.0702	0.0888	0.0856	0.0862	0.0378	0.0785
ES19	0.0863	0.0655	0.0880	0.0624	0.0935	0.0631	0.0845	0.0838	0.0887	0.0878	0.0929	0.0799	0.0747	0.0640	0.0740	0.0792	0.0791	0.0820	0.0494

Table 4. *Cont.*

Total-Relation matrix T for first component of a fuzzy number (u)																			
ES1	0.0883	0.1315	0.1310	0.1290	0.1371	0.1240	0.1313	0.1304	0.1238	0.1335	0.1370	0.1238	0.1356	0.1182	0.1368	0.1209	0.1316	0.1168	0.1237
ES2	0.1180	0.0845	0.1073	0.1136	0.1215	0.1121	0.1260	0.1137	0.1285	0.1281	0.1314	0.1185	0.1299	0.1131	0.1312	0.1183	0.1264	0.1114	0.1303
ES3	0.1332	0.1246	0.0926	0.1218	0.1405	0.1202	0.1342	0.1322	0.1372	0.1373	0.1403	0.1365	0.1385	0.1314	0.1400	0.1370	0.1349	0.1169	0.1390
ES4	0.1303	0.1231	0.1228	0.0887	0.1390	0.1189	0.1329	0.1282	0.1358	0.1352	0.1388	0.1359	0.1371	0.1178	0.1379	0.1356	0.1266	0.1281	0.1376
ES5	0.1254	0.1266	0.1160	0.1242	0.0901	0.1227	0.1264	0.1155	0.1190	0.1210	0.1312	0.1283	0.1204	0.1134	0.1223	0.1192	0.1188	0.1123	0.1220
ES6	0.1313	0.1326	0.1322	0.1299	0.1383	0.0865	0.1224	0.1214	0.1353	0.1354	0.1383	0.1354	0.1366	0.1193	0.1373	0.1277	0.1213	0.1181	0.1363
ES7	0.1150	0.1190	0.1281	0.1165	0.1347	0.1250	0.0870	0.1281	0.1215	0.1317	0.1291	0.1222	0.1328	0.1166	0.1341	0.1220	0.1292	0.1146	0.1327
ES8	0.1334	0.1342	0.1208	0.1315	0.1407	0.1276	0.1217	0.0917	0.1375	0.1374	0.1379	0.1273	0.1387	0.1314	0.1401	0.1371	0.1349	0.1293	0.1384
ES9	0.1285	0.1307	0.1317	0.1192	0.1376	0.1176	0.1218	0.1108	0.0929	0.1345	0.1376	0.1347	0.1359	0.1290	0.1366	0.1344	0.1322	0.1265	0.1276
ES10	0.1154	0.1305	0.1301	0.1278	0.1362	0.1264	0.1303	0.1192	0.1333	0.0915	0.1362	0.1332	0.1243	0.1248	0.1257	0.1303	0.1207	0.1105	0.1350
ES11	0.1298	0.1309	0.1306	0.1209	0.1361	0.1274	0.1240	0.1207	0.1244	0.1243	0.0956	0.1343	0.1356	0.1284	0.1370	0.1341	0.1159	0.1257	0.1353
ES12	0.1167	0.1173	0.1137	0.1141	0.1168	0.1132	0.1196	0.1267	0.1302	0.1199	0.1227	0.0881	0.1313	0.1247	0.1326	0.1286	0.1280	0.1227	0.1316
ES13	0.1162	0.1197	0.1280	0.1159	0.1334	0.1144	0.1282	0.1277	0.1218	0.1311	0.1238	0.1311	0.0905	0.1154	0.1336	0.1309	0.1141	0.1234	0.1261
ES14	0.1236	0.1160	0.1176	0.1129	0.1298	0.1107	0.1142	0.1134	0.1269	0.1169	0.1298	0.1168	0.1181	0.0800	0.1194	0.1266	0.1248	0.1034	0.1197
ES15	0.1229	0.1350	0.1345	0.1323	0.1395	0.1238	0.1220	0.1339	0.1379	0.1378	0.1408	0.1378	0.1391	0.1219	0.0988	0.1376	0.1352	0.1298	0.1397
ES16	0.1305	0.1311	0.1305	0.1291	0.1379	0.1274	0.1224	0.1310	0.1350	0.1351	0.1380	0.1349	0.1262	0.1190	0.1375	0.0928	0.1224	0.1082	0.1366
ES17	0.1194	0.1279	0.1263	0.1255	0.1263	0.1144	0.1279	0.1273	0.1227	0.1221	0.1248	0.1210	0.1327	0.1257	0.1339	0.1211	0.0875	0.1137	0.1330
ES18	0.1181	0.1234	0.1251	0.1201	0.1379	0.1185	0.1304	0.1312	0.1335	0.1247	0.1377	0.1334	0.1348	0.1292	0.1375	0.1347	0.1325	0.0853	0.1366
ES19	0.1316	0.1229	0.1326	0.1203	0.1388	0.1194	0.1320	0.1320	0.1356	0.1349	0.1386	0.1355	0.1282	0.1213	0.1297	0.1353	0.1334	0.1276	0.0956

A stronger causal signal is evident in groundwater depletion (ES6); this shows a D − R of +0.223. As a mild but sustained driver, it affects other stressors such as salinization (ES16), vegetation stress, and crop yield instability. Its persistent pressure on ecological and human systems highlights the need for sustainable water management. Closely related, heatwaves (ES8) show the strongest influence in this group with a D − R value of +0.240, qualifying as a moderate cause. Their wide-ranging impacts from labor productivity loss to increased energy demand and health risks underline the urgency for adaptive infrastructure and early warning systems. Pest and disease outbreaks (ES9), though traditionally seen as effects, display a slight but notable causal role (D − R +0.034), especially in agricultural systems where ecological imbalances are present. Likewise, air pollution (ES14) (D − R +0.040) contributes indirectly to ecosystem degradation and climate stress. Both exhibit weak causal profiles, but their influence should not be underestimated, particularly in urban and peri-urban settings. Based on the results, the most influential stressors are shown in Table 5.

Table 5. Category A: most influential stressors.

Code	Name	D − R (m)	Interpretation
ES1	Temperature Rise	+0.096	Weak Cause
ES3	Drought Frequency	+0.044	Weak Cause
ES4	Flood Events	+0.205	Mild Cause
ES6	Groundwater Depletion	+0.223	Mild Cause
ES8	Heatwaves	+0.240	Moderate Cause
ES9	Pest and Disease Outbreaks	+0.034	Weak Cause
ES14	Air Pollution	+0.040	Weak Cause
ES16	Salinization/Alkalinity	+0.031	Weak Cause
ES18	Digital Infrastructure Gaps	+0.213	Moderate Cause

Salinization and alkalinity (ES16), with a D − R of +0.031, also rank as a weak cause, often emerging from water misuse and poor drainage. Although chronic in nature, their influence is persistent, especially in degrading soil productivity. Finally, digital infrastructure gaps (ES18) are prominent with a D − R of +0.213, marking a moderate and somewhat non-traditional cause in the environmental domain. These gaps hinder access to early warning systems, climate-smart agriculture, and efficient resource use; thereby, weakening the resilience of the entire food and environmental supply chains. Based on the results, a subset of environmental stressors that primarily function as outcomes or consequences of systemic pressures within the environmental system are explored, as shown in Table 6. These stressors, categorized under the effect group, are characterized by negative D − R values, indicating that they are more influenced by other stressors rather than exerting influence themselves.

Based on the results of the Fuzzy DEMATEL analysis, a subset of environmental stressors is identified that primarily function as outcomes or consequences of systemic pressures within the environmental system. These stressors, categorized under the effect group, are characterized by negative D − R values, indicating that they are more influenced by other stressors rather than exerting influence themselves. Soil degradation (ES5) exhibits a D − R value of −0.366, marking it as a moderate effect and one of the most heavily impacted stressors in the system. Soil degradation is typically the result of cumulative upstream drivers such as droughts, poor land management, salinization, and extreme weather patterns. Its high sensitivity to multiple influences highlights its role as a critical indicator of environmental health and productivity, particularly in agricultural and rural

landscapes. Vegetation loss (ES11) and extreme weather events (ES12) also emerge as moderately affected stressors, with D − R values of −0.164 and −0.184, respectively. Vegetation loss reflects a direct consequence of interacting stressors such as temperature rise, pest outbreaks, and groundwater depletion, which jointly weaken ecosystems. Similarly, extreme weather events represent the culmination of climate variability and atmospheric instability driven by broader systemic imbalances such as heatwaves and land use change. Sea level rise (ES13), another moderately influenced stressor (D − R −0.173), is shaped by long-term changes such as global temperature increase and melting ice masses. While it does not significantly affect other stressors in this framework, its implications, such as flooding and coastal displacement, are far-reaching and often irreversible. Cold spells (ES17) also show a moderate effect role (D − R −0.115), indicating their sensitivity to overarching climatic dynamics rather than being major drivers themselves. In contrast, land use change/urban sprawl (ES10) is characterized by a weak effect role with a D − R value of −0.057. While influenced by drivers such as population pressure, economic development, and digital infrastructure gaps, it also has the potential to influence other stressors in return, such as vegetation loss and flood risk, suggesting its dual position in the network.

Table 6. B. Most influenced stressors (effect group, D − R < 0).

Code	Name	D − R (m)	Interpretation
ES5	Soil Degradation	−0.366	Moderate Effect
ES10	Land Use Change/Urban Sprawl	−0.057	Weak Effect
ES11	Vegetation Loss	−0.164	Moderate Effect
ES12	Extreme Weather Events	−0.184	Moderate Effect
ES13	Sea Level Rise	−0.173	Moderate Effect
ES17	Cold Spells	−0.115	Moderate Effect
ES19	Transport and Energy Disruption	+0.006	Balanced

Interestingly, transport and energy disruption (ES19) displays a nearly neutral D − R value of +0.006, placing it in a balanced position between a cause and an effect. This suggests a reciprocal interaction where disruptions in transport and energy systems are both triggered by and contributors to other environmental stressors like extreme weather or infrastructure gaps. Fuzzy DEMATEL also highlights a core group of environmental stressors with the highest D + R values, marking them as the most central and systemically prominent elements within the environmental network. These stressors are deeply embedded in the system through both the influence they exert and the feedback they receive, making them critical leverage points for policy intervention and strategic planning. The stressors are shown in Table 7.

Table 7. Most prominent stressors.

Code	Name	D + R (m)	Role
ES15	Forest Fires	2.961	Central and Balanced
ES19	Transport and Energy Disruption	2.951	Central and Balanced
ES11	Vegetation Loss	2.858	Influenced Prominence
ES16	Salinization/Alkalinity	2.767	Strong Influence
ES9	Pest and Disease Outbreaks	2.832	Strongly Involved

Forest fires (ES15) are projected as the most central and balanced stressor with a D + R value of 2.961. This indicates that forest fires are both heavily influenced by other stressors, such as heatwaves, droughts, and vegetation loss, and exert substantial influence in return by accelerating air pollution, biodiversity loss, and land degradation. Its central and balanced nature means that it both shapes and reflects systemic vulnerabilities, requiring integrated fire management, land use planning, and climate adaptation policies. Transport and energy disruption (ES19), with a D + R value of 2.951, is also categorized as central and balanced. This stressor captures a pivotal position in the infrastructure/climate nexus. It is influenced by extreme weather, digital infrastructure gaps, and sea level rise, while in turn disrupting supply chains, emergency response, and mobility.

Vegetation loss (ES11), with a D + R value of 2.858, signifies a case of influenced prominence. Although it is more affected than being a cause, its centrality reflects its interlinkage with several other drivers and consequences, ranging from drought, land use change to carbon sequestration loss. Salinization and alkalinity (ES16), with a D + R of 2.767, is considered as a strong influencer. It has a substantial role in shaping soil degradation, groundwater stress, and agricultural output, while being moderately affected itself. Its prominence in the network suggests that soil and water management strategies, particularly in arid and semi-arid zones, are essential for mitigating downstream impacts. Lastly, pest and disease outbreaks (ES9) hold a D + R value of 2.832, reflecting strong involvement in both causal and effect pathways. Despite its relatively low D − R (a weak cause), its high total interaction indicates that it is systemically embedded, influenced by climate change, vegetation patterns, and human activity, while also exacerbating agricultural and ecological vulnerabilities. Integrated pest management, surveillance, and climate-smart agricultural practices become vital here.

The visualization showing the strategic classification of environmental stressors across five quadrants based on their D − R (causal strength) and D + R (centrality/prominence) values is shown in Figure 2. Each stressor is plotted and grouped according to its strategic role in the system.

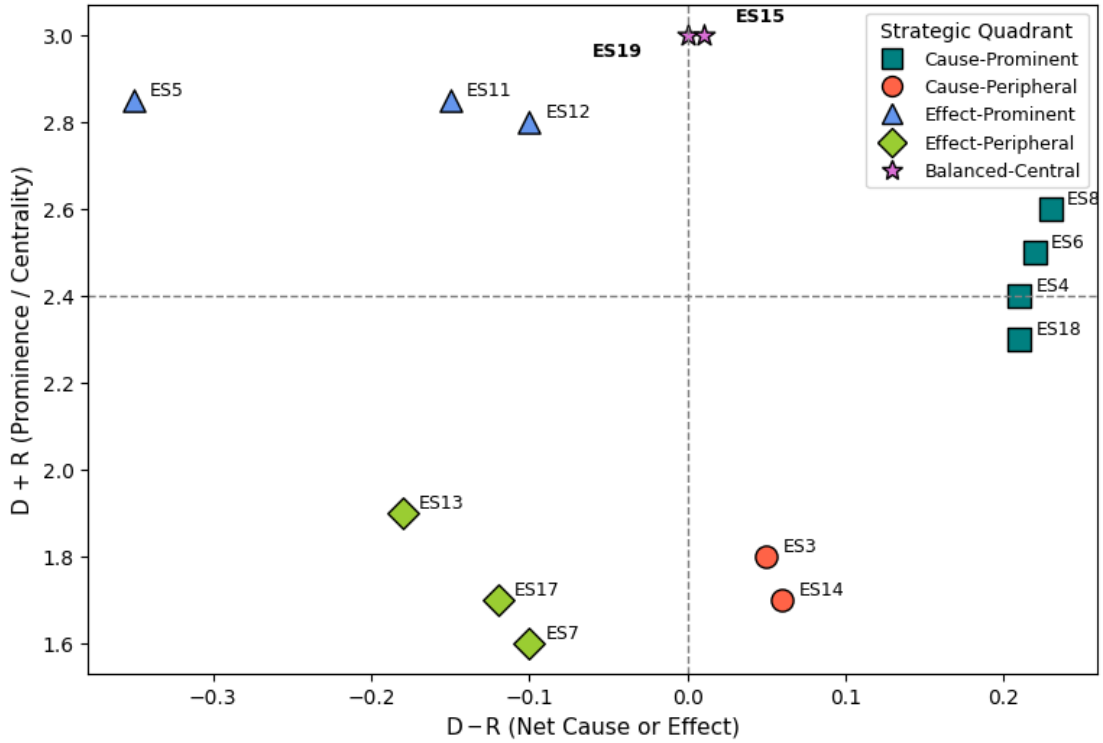

Figure 2. Strategic classification of environment stressors.

4.1. Environmental Stressors Index (ESI)

The ESI is proposed using Equations (10)–(12); this aims to quantify vulnerability of agricultural systems due to environmental stressors. This index assesses how stressors will evolve under RCP 4.5 (moderate scenario) and RCP 8.5 (high emissions scenario) up to 2100. Based on the Fuzzy DEMATEL results, the most influential and prominent stressors ES3, ES8, ES9, ES11, ES14, ES16, ES18, and ES19 are selected. The 19 environmental stressors to the 9 most influential are selected using a threshold based on DEMATEL centrality (D + R), where stressors exceeding the sample mean and belonging to the top quantile of systemic prominence are retained. A stability test with $\pm$10% perturbation of weights confirms the robustness of this selection. The top nine stressors are invariant in $\geq$95% of perturbations, with median Jaccard ≥ 0.90 and median Spearman's $\rho \geq 0.90$, indicating high robustness of the selection to $\pm$10% weight uncertainty. The expert panel comprises 15 specialists (Table 3) with 5–15 years of relevant experience. A Delphi method is employed to consider experts' judgment; a consensus coefficient of Kendall's W = 0.71 is obtained, indicating substantial agreement. Further, pairwise comparisons are expressed as fuzzy triplets (Table 2) and defuzzified using the Center of Area (COA) method to derive crisp weights. This framework ensures that the selection of indicators and weights is auditable, evidence-based, and replicable. Three regions in Uttarakhand are selected as samples to represent distinct agro-climatic zones: Region A, Rudraprayag (central/higher-altitude, hotspot of extreme events); Region B, Udham Singh Nagar (Rudrapur) (terai region, groundwater-stressed); Region C, Almora (mid-Himalaya, rainfall-deficient).

The data shown in Table 8 is obtained from the Climate Atlas of India, Center for Study of Science, Technology, and Policy (CSTEP) Annual Report, 2022, which provides district-level climate variables across India. The time window considered is a short-term period of the 2030s (2021–2050) and is compared with the climate of the near past historical period (1990–2019) at a district level, with a spatial resolution of 1 km $\times$ 1 km grid-based estimates. Missing values are addressed through temporal averaging to maintain data consistency. Normalization ensures consistent directionality: indicators with a positive influence are scaled directly, while those with a negative influence (e.g., extreme temperature anomalies) are reverse-scaled to align interpretation across the dataset.

Table 8. Region-wise stressors.

Region	ES1: Temp Rise (°C)	ES3: Drought Days	ES4: Flood Events	ES6: Groundwater Depth (m)	ES8: Days	ES9: Pest Index	ES14: AQI	ES16: Salinity (EC)	ES18: Internet (%)
Rudraprayag (A)	1.5	30	4	7.0	10	0.7	110	2.5	55
Udham Singh Nagar (B)	1.2	20	2	9.5	12	0.9	140	3.8	35
Almora (C)	1.0	25	3	5.5	8	0.8	100	2.0	60

Source: Climate Atlas of India, Center for Study of Science, Technology, and Policy annual report.

Based on Equations (10) and (11), a normalized matrix is developed as shown in Table 9.

Table 9. Normalized table.

Region	ES1	ES3	ES4	ES6	ES8	ES9	ES14	ES16	ES18
Rudraprayag (A)	1.00	1.00	1.00	0.375	0.50	0.00	0.25	0.28	0.80
Udham Singh Nagar (B)	0.40	0.00	0.00	1.00	1.00	1.00	1.00	1.00	0.00
Almora (C)	0.00	0.50	0.50	0.00	0.00	0.50	0.00	0.00	1.00

The results obtained from normalization show that Rudraprayag shows high vulnerability to climate extremes (heatwaves, floods, temperature, drought) but better infrastructure access whereas Udham Singh Nagar scores high across most stressors (water stress, air pollution, salinity), reflecting a multi-faceted vulnerability profile. Almora demonstrates low exposure except moderate drought and connectivity stress, reflective of its mid-Himalayan character. Using Equations (11) and (12), ESI scores are calculated and shown in Table 10.

Table 10. ESI scores for each region.

Region	ESI Score	Interpretation
Rudraprayag (A)	0.755	Very High Vulnerability (climate-driven and moderate infrastructure gaps)
Udham Singh Nagar (B)	0.715	High Vulnerability (resource and pollution stressors dominate)
Almora (C)	0.435	Moderate Vulnerability (limited climate extremes, but connectivity critical)

The ESI scores are visualized in Figure 3.

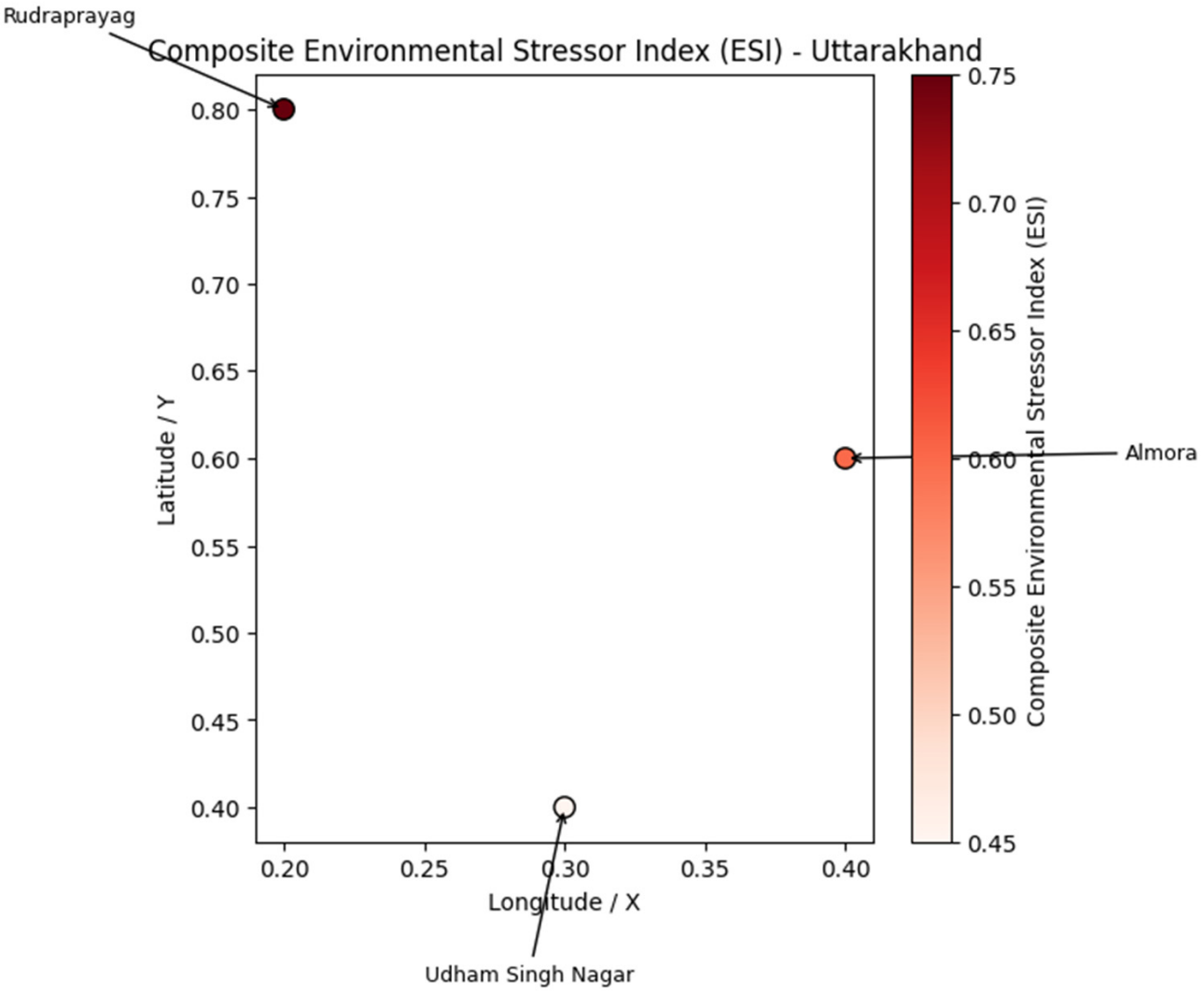

Figure 3. Choropleth map visualizes the ESI.

The choropleth map visualizes the composite Environmental Stressor Index (ESI) across three representative regions in Uttarakhand—Rudraprayag, Udham Singh Nagar, and Almora. The color gradient indicates the intensity of environmental stress, with darker shades representing higher levels of stress and vulnerability. The main results are detailed as follows.

(a) Rudraprayag (ESI: 0.755; High Vulnerability)

Rudraprayag, a high-altitude central Himalayan region, shows the highest composite ESI score. This is due to its exposure to extreme events like floods (ES4), heatwaves (ES8), and landslide-triggering weather conditions. The Fuzzy DEMATEL results support this by identifying stressors such as groundwater depletion (ES6) and heatwaves (ES8) as moderate causes, flood events (ES4) as a mild cause, with forest fires (ES15) and transport/energy disruption (ES19) as central and balanced stressors. The convergence of high causality and high prominence of stressors suggests that Rudraprayag is not only highly exposed but is also a driver node in systemic agricultural vulnerability.

(b) Udham Singh Nagar (ESI: 0.715; Moderate-High Vulnerability)

As a terai region with intensive agriculture, this district faces high stress from groundwater depletion (ES6) and salinization (ES16). Fuzzy DEMATEL results flag both of these as causal stressors, indicating that Udham Singh Nagar's challenges are structural and anthropogenically driven. The ESI score reflects chronic water stress from unsustainable irrigation practices, technological gaps (ES18) in managing these risks, and rising air pollution (ES14) and pest outbreaks (ES9) due to mono-cropping and climate variability. This makes it a priority area for agri-tech and sustainable water management interventions.

(c) Almora (ESI: 0.435; Moderate-Low Vulnerability)

A mid-Himalayan region, Almora shows relatively lower composite environmental stress. However, it remains vulnerable to vegetation loss (ES11), soil degradation (ES5), and extreme weather events (ES12), all identified as effect stressors in the DEMATEL results. These stressors are more a consequence of upstream or system-wide causes rather than internal triggers. Thus, Almora is more reactive than proactive in the environmental stress network. While immediate vulnerabilities are lower, systemic exposure is still significant, especially under future climate scenarios (RCP 4.5/8.5).

To reduce the risk of double-counting correlated stressors, we propose an adjustment in the ESI calculation by introducing a penalty term for collinearity. While the rank ordering of districts remains broadly stable, with Rudraprayag and Udham Singh Nagar both emerging as highly stressed, the adjustments slightly increase Rudraprayag's relative vulnerability while lowering Almora's index. This refinement demonstrates that the ESI is reasonably robust but also highlights the importance of addressing collinearity to avoid overemphasizing overlapping climate shocks (e.g., drought and flood frequency).

4.2. Simulation for RCP 4.5 and RCP 8.5

For future climate projections, data is obtained from the CMIP6 multi-model ensemble, incorporating outputs from ten global climate models to reduce model-specific uncertainties. To address systematic bias, quantile mapping is applied against the IMD baseline climatology (1980–2010) following the ISIMIP protocol, thereby improving the representation of precipitation and temperature distributions. Land surface and soil parameters are derived from the Harmonized World Soil Database (HWSD) and MODIS land cover datasets, with the final datasets downscaled to a $0.25^\circ \times 0.25^\circ$ (~25 km) spatial resolution aligned with IMD gridded records. All projections are regionally calibrated using IMD historical data for Indian districts, ensuring contextual relevance. These projections under RCP 4.5 and RCP 8.5 provide the climatic drivers for ESI simulations. This study incorporates

climate stressor projections from CMIP6 multi-model ensembles under RCP 4.5 and RCP 8.5 scenarios. RCP 4.5 represents a stabilization scenario with moderate mitigation, while RCP 8.5 reflects a business-as-usual pathway with high emissions (Reference: Supplementary Text S1, Tables S1 and S2). ESI Simulation Output for regions under RCP 4.5 and RCP 8.5 is achieved using min–max normalization shown in Table 11.

Table 11. ESI score RCP 4.5 and 8.5.

Region	ESI Score (RCP 4.5)	ESI Score (RCP 8.5)
Udham Singh Nagar	0.711 → Very High Vulnerability	0.529 → Moderate Vulnerability
Rudraprayag	0.511 → Moderate Vulnerability	0.740 → Very High Vulnerability
Almora	0.167 → Low Vulnerability	0.133 → Very Low Vulnerability

Based on the data, a heatmap is made as shown in Figure 4. Environmental stressors under RCP 4.5 show distinct vulnerability profiles across the three regions. Rudraprayag (A) shows very high stress levels across most indicators including temperature rise, drought days, flood events, and moderate stress in groundwater depth and salinity, suggesting a climate-driven vulnerability pattern. Udham Singh Nagar (B) exhibits maximum normalized values across all stressors, especially for heatwave days, pest index, AQI, and salinity, indicating critical stress from resource depletion and environmental degradation; this makes it the most vulnerable region. On the contrary. Almora (C) reflects low to moderate stress, with relatively better performance in key stressors like AQI, salinity, and internet access, implying comparatively lower vulnerability, though drought and pest risks persist. This visualization highlights the need for region-specific climate adaptation strategies based on dominant environmental stress patterns.

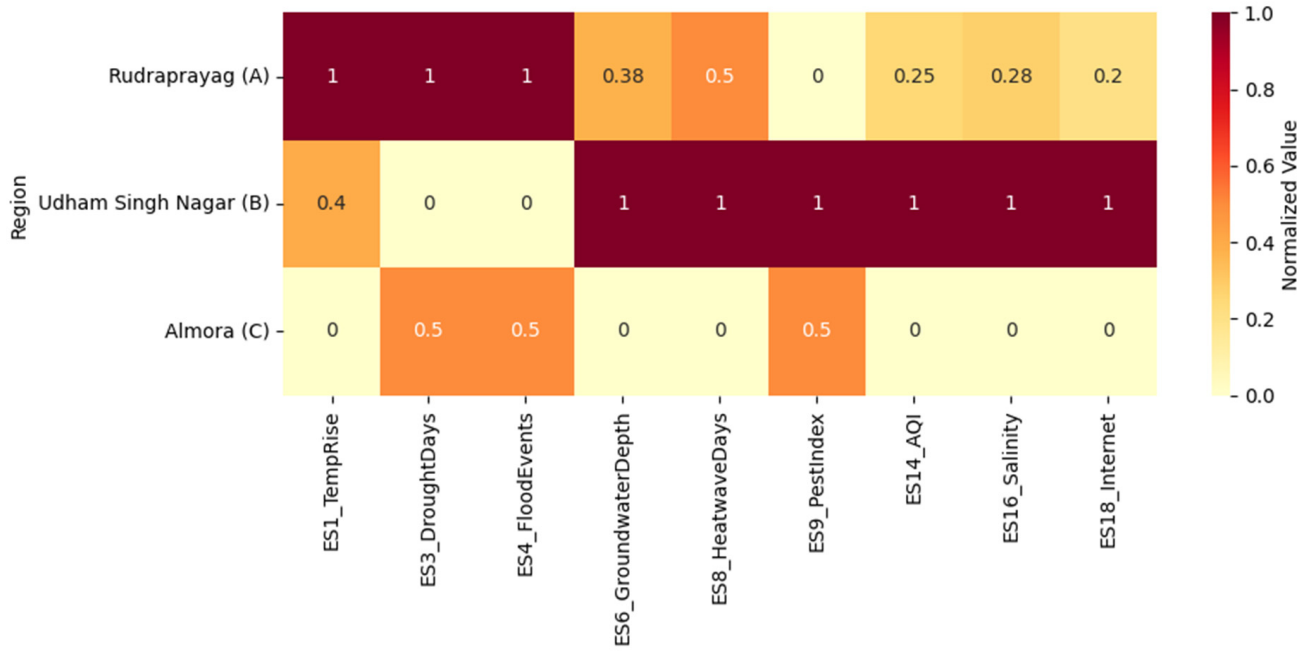

Figure 4. Environmental stressors under RCP 4.5.

The heatmap under the RCP 8.5 scenario is shown in Figure 5. This reveals an intensification of environmental stress across regions, with Udham Singh Nagar (B) remaining under severe vulnerability. The map shows maximum normalized values (1.0) across all stressors, highlighting compounded stress from climate extremes, environmental degradation, and poor infrastructure. Rudraprayag (A) also shows very high stress for temperature

rise, drought, and flood events, with moderate levels for groundwater depth, heatwaves, and salinity, indicating growing climate-induced pressure. On the contrary, Almora (C) continues to experience comparatively lower stress, though moderate vulnerability is still evident for drought, flood, and pest risk. Overall, the RCP 8.5 projection indicates a significant amplification of climate stress, particularly in the lowland regions, demanding urgent adaptive capacity building and mitigation interventions.

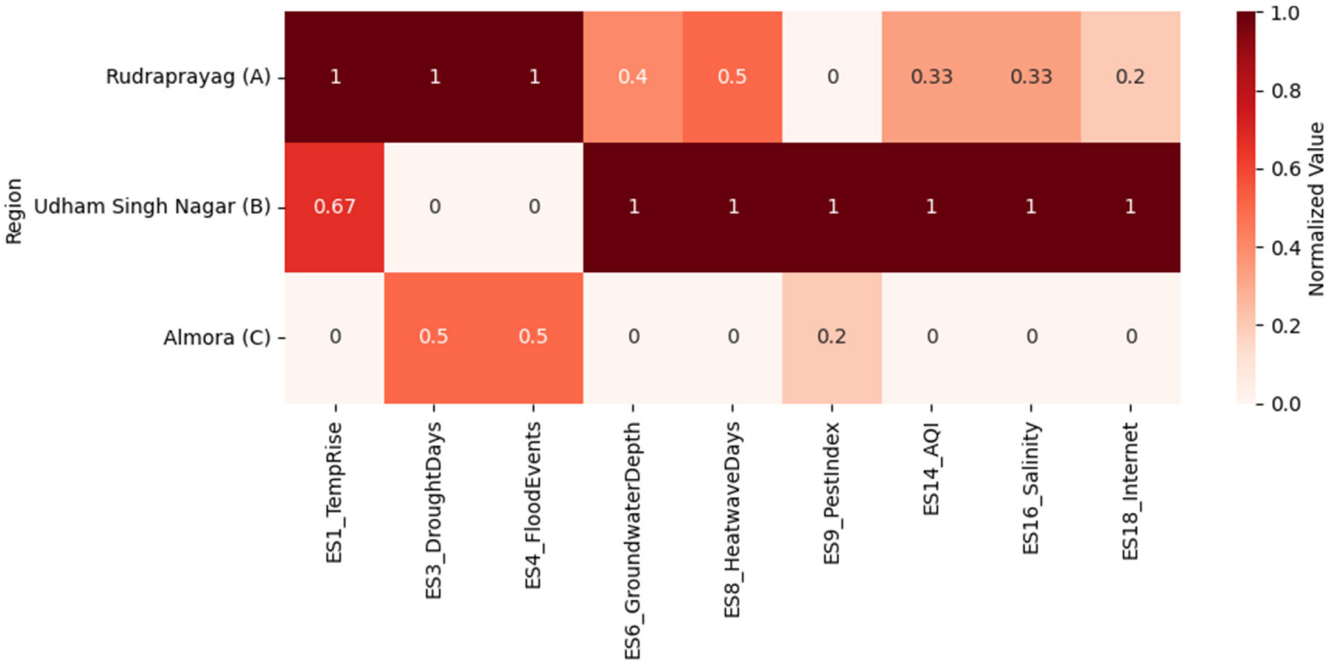

Figure 5. Environmental stressors under RCP 8.5.

To complement the environmental stressor analysis, crop yield models play a critical role in assessing agricultural vulnerability and food insecurity under climate change scenarios like RCP 4.5 and RCP 8.5. These models integrate climate variables such as temperature rise, rainfall variability, drought frequency, and heatwaves with crop-specific physiological responses to estimate yield fluctuations over time. By simulating crop performance under projected stress conditions, models like Decision Support System for Agrotechnology Transfer (DSSAT) or AquaCrop can identify regions where food production is at risk, supporting the formulation of targeted adaptation strategies.

This approach provides a quantitative basis to evaluate the impact of climate stress on food availability, helping to prioritize climate-smart agricultural interventions, enhance resilience planning, and mitigate food insecurity, especially in ecologically sensitive districts like Rudraprayag and Udham Singh Nagar.

4.3. Bridging Environmental Stress to Food Supply Chain Insecurity

Ultimately, each environmental stressor, whether biophysical such as soil degradation or socio-technical such as lack of ICT, cascades into FSC vulnerability. The dual insights from Fuzzy DEMATEL (causal structure) and ESI (regional intensity) help stakeholders predict, prevent, and absorb shocks across the entire food system. The impact of environmental stressors on food supply chain stages is shown in Figure 6.

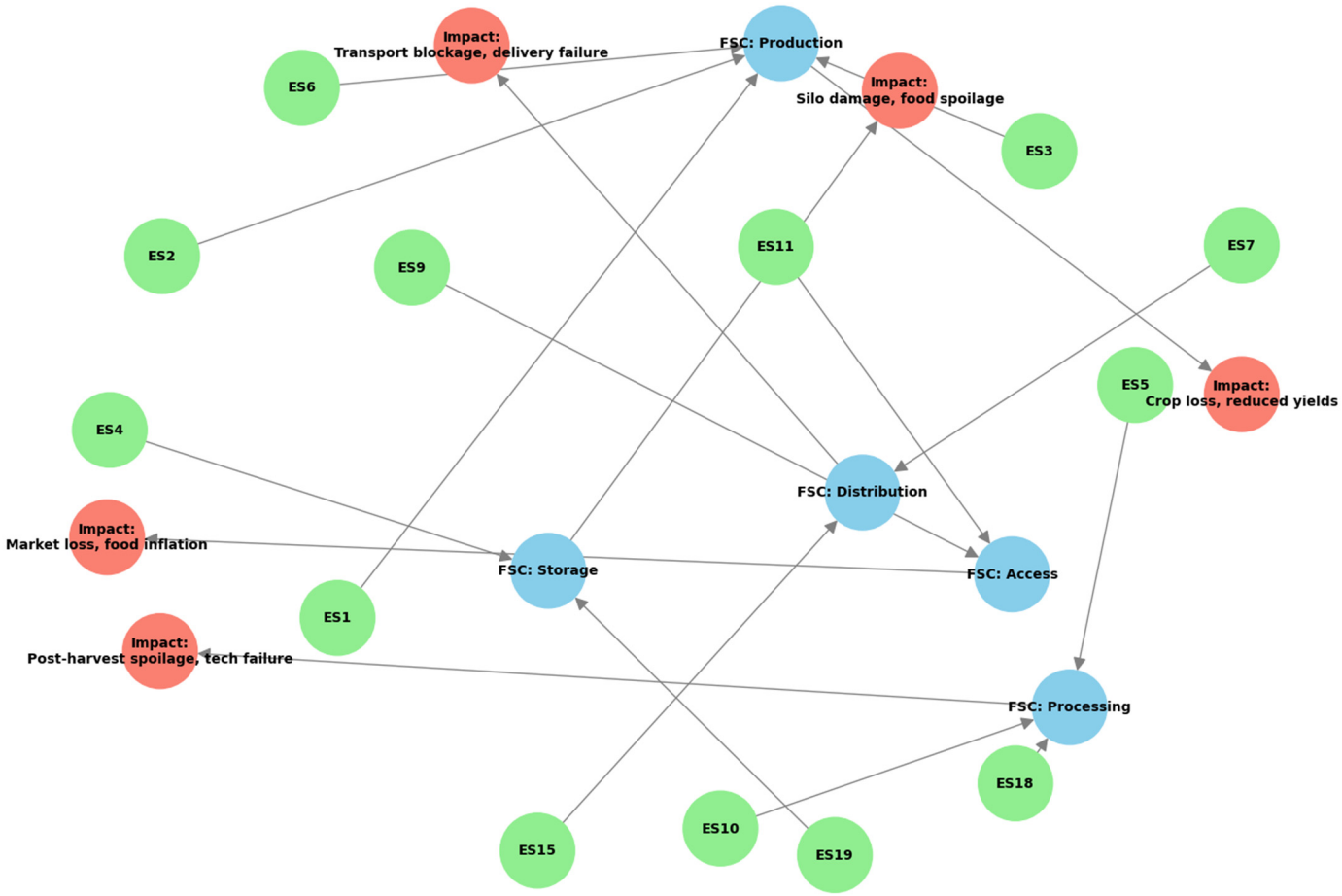

Figure 6. Impact of environmental stressors on food supply chain stages.

The results can be validated against historical socio-economic and disaster records. For example, Rudraprayag has consistently faced recurrent flooding and landslide events (notably the 2013 Kedarnath floods), which aligns with its high ESI score driven by flood and groundwater stressors. Udham Singh Nagar, in contrast, has recorded serious air pollution, irrigation pressures, and groundwater depletion in state monitoring reports, consistent with its elevated stressor profile from AQI, salinity, and pest index. Almora, while recording lower overall stress, has experienced recurrent droughts and market access challenges due to its hilly terrain and limited connectivity, reflecting its ESI score on drought days and internet penetration. This triangulation with observed losses and vulnerabilities supports the validity of ESI as a diagnostic tool, while also highlighting district-specific stress patterns.

As can be seen from the results, Rudraprayag district is vulnerable to environmental stressors, particularly landslides and flash floods. The current study aligns with [40], in which deep learning and machine learning models were employed to assess landslide susceptibility across Uttarakhand, identifying Rudraprayag as a high-risk area due to its geological and anthropogenic factors. Moreover, ref. [41] applied multi-criteria decision-making and machine learning techniques for landslide susceptibility evaluation, reinforcing the district's vulnerability. Ref. [42] conducted integrated assessments of flash flood risks in the Upper Ganga Basin, emphasizing that Rudraprayag, alongside Chamoli, experiences recurrent flash floods. Geomorphic studies by [42] underscored the destabilizing effects of dissected topography and unscientific hill cutting on slope stability. Ref. [42] identified the Chamoli District of Uttarakhand where Geographical Information System (GIS)-based susceptibility mapping plays a critical role in identifying vulnerable areas.

Studies conducted by [40–45] exemplify the application of advanced analytical techniques to address landslide susceptibility and related soil erosion and water resource management challenges in Uttarakhand and other areas. Collectively, these studies corroborate the ESI results and highlight the need for district-specific adaptation strategies focusing on disaster preparedness, resilient infrastructure, and sustainable land-use planning [14].

Based on the results, the major findings can be summarized as follows. Firstly, the Environmental Stressor Index (ESI) identifies Udham Singh Nagar as the most consistently vulnerable district, where compounded stressors including water scarcity, salinity, and air pollution intensify risks under both RCP 4.5 and 8.5 scenarios. Secondly, Rudraprayag shows high exposure to floods, droughts, and heatwaves, with vulnerability projected to intensify under the high-emission pathway. Thirdly, Almora remains relatively less vulnerable, yet persistent drought and connectivity limitations indicate risks that cannot be overlooked. These findings suggest significant policy implications such as adaptation must be district-specific, emphasizing water resource management and pollution control in Udham Singh Nagar, resilient infrastructure and early warning systems in Rudraprayag, and drought-resilient cropping in Almora. Broadly, the results highlight the urgency for integrated climate adaptation policies that combine water management, climate-smart agriculture, and digital early warning systems to enhance the resilience of food supply chains at both regional and global levels.

5. Implications

The integration of Fuzzy DEMATEL with a composite ESI provides a holistic, systems-based approach to assess the interconnected nature of climate and environmental stressors impacting agricultural stability. The implications of this dual-framework are extensive, enabling evidence-based decision-making across scales from grassroot agripreneurs to policymakers. This framework not only quantifies region-wise vulnerability but also discloses causal hierarchies among stressors. The implications, particularly in securing food supply chains under current and projected climate scenarios (RCP 4.5 and RCP 8.5), are significant for policymakers, agripreneurs, planners, and researchers.

(a) Integrating ESI into Climate-Smart Agriculture (CSA) Policies

The current Climate-Smart Agriculture (CSA) policies are general in nature. The integration of Fuzzy DEMATEL and ESI enable policymakers to design decentralized, targeted CSA policies which are more relevant to particular conditions of each region. For example, regions with stressors like groundwater depletion and salinization as root causes (e.g., Udham Singh Nagar) should have tailored schemes promoting micro-irrigation, water budgeting, and soil health monitoring. This leads to smarter subsidy allocation and performance-based policy design under schemes such as PMKSY or MGNREGA.

(b) Precision Targeting of Climate Interventions

One of the most significant policy-level implications lies in the capacity to prioritize geographic regions based on composite stressor vulnerability. With ESI quantifying region-specific vulnerability and Fuzzy DEMATEL revealing causal linkages among stressors, governments can triage resources more efficiently. For instance, Rudraprayag, with a high ESI score and multiple cause-prominent stressors, demands immediate investment in flood prevention infrastructure, early warning systems for heatwaves, and reforestation initiatives. Conversely, Almora, with lower vulnerability and more effect-based stressors, may benefit more from long-term ecological restoration.

(c) Targeted Mitigation of Production Disruptors

Regions like Rudraprayag, with high ESI scores, are exposed to intense environmental stressors such as extreme weather events (ES1), floods (ES4), and heatwaves (ES3). These

stressors disrupt sowing windows, reduce crop yields, and degrade soil quality, threatening the very first node of the food supply chain, i.e., agricultural production. Policies must focus on the specific needs of the region. They must include prioritizing region-specific crop insurance and resilient seed varieties, launching district-level early warning systems and emergency procurement measures to buffer FSC shocks, as well as enhancement for farmer coverage under schemes like PMFBY with dynamic premiums based on ESI severity.

(d) Strengthening Infrastructure at Processing and Storage Nodes

High-impact stressors such as infrastructure damage (ES19) and land degradation (ES5), identified as effect-prominent in hilly districts, cause delays and losses in post-harvest processing and storage—critical mid-chain operations. Government programs such as Pradhan Mantri Kisan SAMPADA Yojana (PMKSY) must integrate ESI scores to (a) locate processing hubs in lower-stress areas and (b) climate-proof storage infrastructure (cold chains, silos) using stressor-informed designs.

(e) Tailored Agribusiness Models for Regional Risk Profiles

The ESI framework offers agripreneurs critical foresight to customize inputs, services, and logistics. At the outset, in Udham Singh Nagar, where groundwater depletion (ES2) and salinization (ES6) dominate, startups can deploy soil-moisture sensors, desalinization kits, and promote aquifer recharge solutions. In Almora, mid-altitude farming is affected by rainfall variability (ES7) and pest outbreaks (ES9). Agribusinesses can introduce mobile pest advisory apps, rain-fed crop bundles, biofertilizer dissemination platforms, and adaptive land-use planning.

(f) Institutionalizing Environmental Intelligence Systems

Policymakers must institutionalize stressor monitoring through national dashboards and environmental intelligence systems. Integration of remote sensing, climate models, and AI analytics into public decision-making can facilitate real-time responsiveness to cause-prominent stressors like groundwater depletion or forest fires. Such systems should be made transparent and publicly accessible to enhance accountability.

(g) Public Communication and Behavioral Change Campaigns

The cause-peripheral and effect-peripheral stressors such as air pollution (ES14), sea-level rise (ES13), and cold spells (ES17) often receive less attention due to their lower centrality. However, their localized impact can be severe. Policymakers should deploy targeted communication strategies such as radio broadcasts, school curricula, and mobile advisories, to raise awareness and influence community behavior in these areas. The quadrant-based interpretation of environmental stressors provides a high-resolution, actionable lens for policy formulation. It moves beyond generic climate risk frameworks and enables adaptive governance rooted in data and systems thinking. Policymakers who align their strategies with these insights can build more resilient, equitable, and sustainable food systems for future generations.

Based on the ESI, actionable policies can be mapped to tiered thresholds and tailored to district-specific profiles. Udham Singh Nagar (high vulnerability, ESI > 0.70) requires urgent water resource management through aquifer recharge, strict groundwater regulation, and micro-irrigation, alongside air pollution control and residue management under the National Clean Air Programme; there needs to be promotion of heat- and salinity-tolerant crop varieties. Rudraprayag (high–moderate vulnerability, ESI $\approx$ 0.60–0.70) demands investments in flood-resilient infrastructure and digital early warning systems, expanded PMFBY coverage with ESI-based premiums, and ecosystem restoration for slope stabilization. Almora (moderate–low vulnerability, ESI < 0.50) should prioritize drought-resilient

cropping systems, integrated pest management, and improvements in cold chain connectivity to safeguard post-harvest processes.

For policy implications across key domains, this study underscores targeted pathways. In agriculture, there is a need to promote climate-resilient crops, precision farming, and dynamic insurance schemes. In water resources, there is a need to strengthen groundwater management, micro-irrigation, and watershed control. In biodiversity and ecosystems, there must be expanding afforestation, agroforestry, and digital early warning systems. In infrastructure and agribusiness, climate-proofing cold chains, strategically locating processing hubs, and fostering region-specific agripreneurship models are required. In governance, it is necessary to develop real-time environmental intelligence dashboards, thus ensuring transparency and raising public awareness. Collectively, these structured strategies operationalize the research objectives (RO1–RO3), align with existing national schemes, and advance India's commitments under the Paris Agreement and SDGs, while offering adaptable lessons for other climate-sensitive regions globally.

6. Conclusions, Limitations, and Future Directions for Research

This study provides clear evidence of how increasing climate variability, driven by interconnected environmental stressors, is restructuring food security in vulnerable regions of India. Using the Fuzzy DEMATEL method, it classifies the most influential stressors and constructs a region-specific Environmental Stressor Index (ESI), offering a robust framework to quantify and compare district-level vulnerabilities. The comparative analysis of Rudraprayag, Udham Singh Nagar, and Almora underscores the heterogeneous nature of risks, with exposures spanning climate extremes, hydrological challenges, and pollution pressures. Projections under RCP 4.5 and 8.5 scenarios highlight the urgency of regionally tailored strategies, with Udham Singh Nagar emerging as a critical hotspot due to its multifactorial vulnerabilities. The novelty of this research lies in its integration of causal stressor analysis with crop yield simulations, advancing a systems-level approach that directly links environmental risks to agricultural productivity outcomes. The current study advances the frontier of climate–food security research and provides a transferable framework for other climate-sensitive regions. Continued investigation in this area is vital to strengthen adaptive capacity, safeguard food systems, and support India's commitments under the Paris Agreement and the SDGs.

Despite its comprehensive framework, this study has some limitations. Firstly, the environmental stressors considered are primarily based on existing datasets, which may not fully capture localized microclimatic variations socio-environmental dynamics. Secondly, while Fuzzy DEMATEL effectively models causal relationships among stressors, the analysis does not account for dynamic feedback loops or temporal shifts in stressor influence over time. While the ESI highlights regions with higher composite vulnerability, it does not capture how stress intensities might evolve through feedback or interdependent dynamics over time. Future research could close this gap by extending the index with network-based propagation mechanisms or dynamic modeling approaches. This study applies the ESI framework to three districts in Uttarakhand (Rudraprayag, Udham Singh Nagar, and Almora); the selection is intended primarily as a methodological demonstration and exploratory case study. More extensive datasets and additional districts could provide a more comprehensive assessment of food system vulnerability. Also, this study has an absence of explicit uncertainty quantification and robustness analysis. While stability checks with $\pm 10\%$ perturbation of weights are conducted, the analysis does not capture the full range of uncertainties arising from expert disagreement, indicator measurement error, scenario assumptions, or model structural limitations. Future work can therefore extend the framework through Monte Carlo and bootstrap simulations or sensitivity analysis to

evaluate the stability of the ESI. Additionally, the simulation-based crop yield assessments are sensitive to model parameters and may not fully represent future adaptation responses from farming communities.

Future research should explore integrating temporal models and feedback systems to capture evolving stressor interactions under climate uncertainty. Expanding the geographic scope beyond Uttarakhand and including more granular data (e.g., at block or village level) would enhance spatial precision. Further, incorporating socio-economic resilience indicators including livelihood diversification, adaptive capacity, and governance effectiveness will provide a more holistic understanding of food system vulnerabilities.

Supplementary Materials: The following supporting information can be downloaded at: https://www.mdpi.com/article/10.3390/earth6040121/s1, Supplementary Text S1: Validation of Model Components; Supplementary Table S1: Indicator details; Supplementary Table S2: Defuzzification scores.

Author Contributions: Conceptualization, M.S.; data curation, T.J.; investigation, M.S.; visualization, S.J.; writing—original draft, M.S.; writing—review and editing, S.J., P.G., and T.J. All authors have read and agreed to the published version of the manuscript.

Funding: This research received no external funding.

Institutional Review Board Statement: Ethical approval for this study was obtained from the Research Ethics committee with Reference no. GEU/DOMS/00-20-25/12.

Informed Consent Statement: Informed consent was obtained from all individual participants included in the survey of this study.

Data Availability Statement: The data used in this study is obtained from publicly available and government-recognized sources. Climate projections were obtained from the CMIP6 multi-model ensemble. Historical climate and agro-environmental data were sourced from the Indian Meteorological Department (IMD), Central Ground Water Board (CGWB), Central Pollution Control Board (CPCB), and the Telecom Regulatory Authority of India (TRAI).

Conflicts of Interest: The authors declare no conflict of interest.

References

1. Iqbal, B.; Alabbosh, K.F.; Jalal, A.; Suboktagin, S.; Elboughdiri, N. Sustainable food systems transformation in the face of climate change: Strategies, challenges, and policy implications. *Food Sci. Biotechnol.* **2025**, *34*, 871–883. [CrossRef] [PubMed]
2. Khatri, P.; Kumar, P.; Shakya, K.S.; Kirlas, M.C.; Tiwari, K.K. Understanding the intertwined nature of rising multiple risks in modern agriculture and food system. *Environ. Dev. Sustain.* **2024**, *26*, 24107–24150. [CrossRef]
3. Onyeaka, H.; Nwauzoma, U.M.; Akinsemolu, A.A.; Tamasiga, P.; Duan, K.; Al-Sharify, Z.T.; Siyanbola, K.F. The ripple effects of climate change on agricultural sustainability and food security in Africa. *Food Energy Secur.* **2024**, *13*, e567. [CrossRef]
4. Heydari, M. Cultivating sustainable global food supply chains: A multifaceted approach to mitigating food loss and waste for climate resilience. *J. Clean. Prod.* **2024**, *442*, 141037. [CrossRef]
5. Senthilnathan, S.; Benson, D.; Prasanna, V.; Mallick, T.; Thiyagarajan, A.; Ramasamy, M.; Sundaram, S. Impact of Climate Variability on Maize Yield Under Different Climate Change Scenarios in Southern India: A Panel Data Approach. *Earth* **2025**, *6*, 16. [CrossRef]
6. Lesk, C.; Anderson, W.; Rigden, A.; Coast, O.; Jägermeyr, J.; McDermid, S.; Davis, K.F.; Konar, M. Compound heat and moisture extreme impacts on global crop yields under climate change. *Nat. Rev. Earth Environ.* **2022**, *3*, 872–889. [CrossRef]
7. Climate Change 2022: Impacts, Adaptation and Vulnerability. Available online: https://www.ipcc.ch/report/sixth-assessment-report-working-group-ii/ (accessed on 1 June 2025).
8. Neupane, D.; Adhikari, P.; Bhattarai, D.; Rana, B.; Ahmed, Z.; Sharma, U.; Adhikari, D. Does climate change affect the yield of the top three cereals and food security in the world? *Earth* **2022**, *3*, 45–71. [CrossRef]
9. Hafeez, A.; Batool, R.; Arshad, A.; Khan, M.N.; Ali, S.; Singh, N.; Garhwal, V.; Javed, M.A.; Fatima, E.; Suleman, F.; et al. Soil and water conservation under changing climate. In *Challenges and Solutions of Climate Impact on Agriculture*; Academic Press: Cambridge, MA, USA, 2025; pp. 307–328.
10. Raj, S.; Roodbar, S.; Brinkley, C.; Wolfe, D.W. Food security and climate change: Differences in impacts and adaptation strategies for rural communities in the global south and north. *Front. Sustain. Food Syst.* **2022**, *5*, 691191. [CrossRef]

11. Khan, S.A.R.; Razzaq, A.; Yu, Z.; Shah, A.; Sharif, A.; Janjua, L. Disruption in food supply chain and undernourishment challenges: An empirical study in the context of Asian countries. *Socio-Econ. Plan. Sci.* **2022**, *82*, 101033. [CrossRef]
12. OECD-FAO Agricultural Outlook 2023–2032. Available online: https://www.oecd.org/en/publications/oecd-fao-agricultural-outlook-2023-2032_08801ab7-en/full-report/regional-briefs_adcb9fec.html (accessed on 1 June 2025).
13. CSTEP. Annual Report 2022–2023. Available online: https://cstep.in/publications-details.php?id=2535 (accessed on 1 June 2025).
14. Kumar, A.; Giri, R.K.; Taloor, A.K.; Singh, A.K. Rainfall trend, variability and changes over the state of Punjab, India 1981–2020: A geospatial approach. *Remote Sens. Appl. Soc. Environ.* **2021**, *23*, 100595. [CrossRef]
15. Halder, P.; Dey, R.K.; Mandal, S. Long-period trend analysis of annual and seasonal rainfall in West Bengal, India (1901–2020). *Theor. Appl. Climatol.* **2023**, *154*, 685–703. [CrossRef]
16. Chakraborty, D.; Roy, A.; Singh, N.U.; Saha, S.; Das, S.K.; Mridha, N.; Yumnam, A.; Paul, P.; Gowda, C.; Biam, K.P.; et al. Assessing Climate Change Impact on Rainfall Patterns in Northeastern India and Its Consequences on Water Resources and Rainfed Agriculture. *Earth* **2025**, *6*, 2. [CrossRef]
17. Vijayakumar, S.; Nayak, A.K.; Ramaraj, A.P.; Swain, C.K.; Geethalakshmi, V.; Pazhanivelan, S.; Tripathi, R.; Sudarmanian, N.S. Rainfall and temperature projections and their impact assessment using CMIP5 models under different RCP scenarios for the eastern coastal region of India. *Curr. Sci.* **2021**, *121*, 222–232. [CrossRef]
18. Mishra, V.; Kumar, D.; Ganguly, A.R. Climate change and India: Temperature and precipitation trends. *Nat. Clim. Change* **2020**, *10*, 389–390.
19. Roxy, M.K.; Ghosh, S.; Pathak, A.; Athulya, R.; Krishnan, R. A threefold rise in extreme rainfall events over central India. *Nat. Commun.* **2017**, *8*, 708. [CrossRef]
20. Sharma, T.; Mujumdar, P.P. Increasing frequency and spatial extent of concurrent meteorological droughts and heatwaves in India. *Sci. Rep.* **2017**, *7*, 15582. [CrossRef]
21. Singh, S.; Jain, V.; Goyal, M.K. Evaluating climate shifts and drought regions in the central Indian river basins. *Sci. Rep.* **2025**, *15*, 29701. [CrossRef]
22. National Action Plan to Combat Desertification and Land Degradation Through Forestry Interventions. Available online: https://moef.gov.in/uploads/2023/07/NAP%20final-2023.pdf (accessed on 1 June 2025).
23. Minhas, P.S. Saline water management for agriculture in India. *Agric. Water Manag.* **1996**, *30*, 1–21. [CrossRef]
24. Choudhury, U.; Singh, S.K.; Kumar, A.; Meraj, G.; Kumar, P.; Kanga, S. Assessing land use/land cover changes and urban heat island intensification: A case study of Kamrup Metropolitan District, Northeast India (2000–2032). *Earth* **2023**, *4*, 503–521. [CrossRef]
25. Sati, V.P. Cropping Patterns and Change. In *Farming Systems and Sustainable Agriculture in the Himalaya*; Springer Nature: Cham, Switzerland, 2024; pp. 23–38.
26. World Resources Institute. *Aqueduct Water Risk Atlas*; World Resources Institute: Washington, DC, USA, 2019.
27. Yadav, R.K.; Rai, S.C.; Khan, M.R.; Shree, K. Drought's silent symphony and unmasking the invisible weight on human life in Chhatarpur of Bundelkhand Region, India. *Clim. Change* **2025**, *178*, 51. [CrossRef]
28. Ravindra, K.; Bhardwaj, S.; Ram, C.; Goyal, A.; Singh, V.; Venkataraman, C.; Bhan, S.C.; Sokhi, R.S.; Mor, S. Temperature projections and heatwave attribution scenarios over India: A systematic review. *Heliyon* **2024**, *10*, e26431. [CrossRef]
29. Norgate, M.; Tiwari, P.R.; Das, S.; Kumar, D. On the heat waves over India and their future projections under different SSP scenarios from CMIP6 models. *Int. J. Climatol.* **2024**, *44*, 973–995. [CrossRef]
30. Patra, S.; Kumar, A.; Saikia, P. Deforestation and forests degradation impacts on livelihood security and climate change: Indian initiatives towards its mitigation. In *Environmental Degradation: Challenges and Strategies for Mitigation*; Springer International Publishing: Cham, Switzerland, 2022; pp. 371–392.
31. Guria, R.; Mishra, M.; Baraj, B.; Goswami, S.; Santos, C.A.G.; da Silva, R.M.; Bhutia, K.D.O. Examining the drivers of forest cover change and deforestation susceptibility in Northeast India using multicriteria decision-making models. *Environ. Monit. Assess.* **2024**, *196*, 1098. [CrossRef]
32. Mina, U.; Dimri, A.P.; Farswan, S. Forest fires and climate attributes interact in central Himalayas: An overview and assessment. *Fire Ecol.* **2023**, *19*, 14. [CrossRef]
33. Stavi, I.; Thevs, N.; Priori, S. Soil salinity and sodicity in drylands: A review of causes, effects, monitoring, and restoration measures. *Front. Environ. Sci.* **2021**, *9*, 712831. [CrossRef]
34. Rafie-Rad, Z.; Raza, T.; Eash, N.S.; Moradi-Khajevand, M.; Moradkhani, M. Effects of outdoor air pollutants on plants and agricultural productivity. In *Health and Environmental Effects of Ambient Air Pollution*; Academic Press: Cambridge, MA, USA, 2024; pp. 71–90.
35. Yadav, S.; Korat, J.R.; Yadav, S.; Mondal, K.; Kumar, A.; Kumar, S.; Kumar, S. Impacts of climate change on fruit crops: A comprehensive review of physiological, phenological, and pest-related responses. *Int. J. Environ. Clim. Change* **2023**, *13*, 363–371. [CrossRef]

36. Morkūnas, M.; Rudienė, E.; Ostenda, A. Can climate-smart agriculture help to assure food security through short supply chains? A systematic bibliometric and bibliographic literature review. *Bus. Manag. Econ. Eng.* **2022**, *20*, 207–223.
37. Wei, F.; Koc, E.; Li, N.; Soibelman, L.; Wei, D. A data-driven framework to evaluate the indirect economic impacts of transportation infrastructure disruptions. *Int. J. Disaster Risk Reduct.* **2022**, *75*, 102946. [CrossRef]
38. Seifi, N.; Ghoodjani, E.; Majd, S.S.; Maleki, A.; Khamoushi, S. Evaluation and prioritization of artificial intelligence integrated block chain factors in healthcare supply chain: A hybrid Decision Making Approach. *Comput. Decis. Mak. Int. J.* **2025**, *2*, 374–405.
39. Bhattacharya, S.; Ali, T.; Chakravortti, S.; Pal, T.; Majee, B.K.; Mondal, A.; Pande, C.B.; Bilal, M.; Rahman, M.T.; Chakrabortty, R. Application of Machine Learning and Deep Learning Algorithms for Landslide Susceptibility Assessment in Landslide Prone Himalayan Region. *Earth Syst. Environ.* **2024**, *9*, 1427–1445. [CrossRef]
40. Chauhan, V.; Gupta, L.; Dixit, J. Landslide susceptibility assessment for Uttarakhand, a Himalayan state of India, using multi-criteria decision making, bivariate, and machine learning models. *Geoenviron. Disasters* **2025**, *12*, 2. [CrossRef]
41. Pandey, P.; Chauhan, P.; Bhatt, C.M.; Thakur, P.K.; Kannaujia, S.; Dhote, P.R.; Roy, A.; Kumar, S.; Chopra, S.; Bhardwaj, A.; et al. Cause and process mechanism of rockslide triggered flood event in Rishiganga and Dhauliganga River Valleys, Chamoli, Uttarakhand, India using satellite remote sensing and in situ observations. *J. Indian Soc. Remote Sens.* **2021**, *49*, 1011–1024. [CrossRef]
42. Khanduri, S.; Sajwan, K.S.; Rawat, A.; Dhyani, C.; Kapoor, S. Disaster in Rudraprayag District of Uttarakhand Himalaya: A special emphasis on geomorphic changes and slope instability. *J. Geogr. Nat. Disasters* **2018**, *8*, 1–9.
43. Rihan, M.; Talukdar, S.; Naikoo, M.W.; Ahmed, R.; Shahfahad; Rahman, A. Improving landslide susceptibility prediction in Uttarakhand through hyper-tuned artificial intelligence and global sensitivity analysis. *Earth Syst. Environ.* **2024**, 1–20.
44. Nawazuzzoha, M.; Rashid, M.; Iqbal, F.; Suheb; Bhardwaj, A.; Shakeel, A.; Arabameri, A.; Naqvi, H.R. Advanced Machine Learning Models for Landslide Susceptibility Mapping in South Sikkim Himalayas, India. *Geol. J.* 2025, *in press*. [CrossRef]
45. Prajapati, D.K.; Choudhary, M.; Avtar, R.; Singh, S.; Alsulamy, S.; Kharrazi, A. Transformative Spatio-Temporal Insights into Indian Summer Days for Advancing Climate Resilience and Regional Adaptation in India. *Earth* **2025**, *6*, 39. [CrossRef]